Step response of a Mariner class hullform in pitch and heave

Hines, Dean H.; Gies, Leo C.

Massachusetts Institute of Technology

STEP RESPONSE OF A MARINER CLASS HULLFORM IN PITCH AND HEAVE

by
Dean H. Hines, Lieutenant, US Navy
and
Leo C. Gies, Lieutenant, US Navy
Supervisor: Prof. J. E. Kerwin

STEP RESPONSE OF A MARINER CLASS HULLFORM IN PITCH AND HEAVE

by

DEAN H. HINES, LIEUTENANT, U.S. NAVY
B.S., UNITED STATES NAVAL ACADEMY
(1957)

and

LEO C. GIES, LIEUTENANT, U.S. NAVY
B.S., UNITED STATES NAVAL ACADEMY
(1958)

SUBMITTED IN PARTIAL FULFILLMENT OF THE REQUIREMENTS
FOR THE DEGREE OF
NAVAL ENGINEER AND MASTER OF SCIENCE
IN NAVAL ARCHITECTURE AND MARINE ENGINEERING
at the
MASSACHUSETTS INSTITUTE OF TECHNOLOGY
June 1965

STEP RESPONSE OF A MARINER CLASS HULLFORM IN PITCH AND HEAVE

by

Dean H. Hines

and

Leo C. Gies

Submitted to the Department of Naval Architecture and Marine Engineering on May 21, 1965 in partial fulfillment of the requirements for the degree of Naval Engineer and the degree of Master of Science in Naval Architecture and Marine Engineering.

ABSTRACT

In its motion response to a disturbance, a ship can be closely approximated as a second order system. The solution of these second order equations is used to determine the motion stability of the ship. By applying a step disturbance to a ship model and measuring the response, the linearity can be used to find the response to any disturbance.

In this work a step disturbance was applied to a Mariner class hullform and the response measured. From this response the response to regular sinusoidal excitations was computed. The response to the sinusoidal inputs was then used to determine the coefficients of virtual inertia and damping for the Mariner in pitch and heave.

The derived results at zero speed were compared with values computed by strip theory.

THESIS SUPERVISOR: J. E. Kerwin
TITLE: Associate Professor of Naval Architecture

ACKNOWLEDGEMENTS

The authors wish to thank Professor J. E. Kerwin for his continual advice and encouragement during this project.

The authors also wish to thank Mr. Frank Sellars for his support, especially in obtaining the analog to digital conversion of the data.

The assistance of Commander W. R. Porter was highly beneficial in obtaining the theoretical results.

The assistance of Mr. H. der Kinderen in performing the experimental work was greatly appreciated.

This work was done in part by the computation center at the Massachusetts Institute of Technology, Cambridge, Massachusetts.

TABLE OF CONTENTS

INDEX OF TABLES

INDEX OF FIGURES

CHAPTER I

INTRODUCTION

The equations of ship motion developed by Abkowitz (1) are a linearized set of second order partial differential equations. In the vertical plane the equations are

$$(m-Z_{\ddot{z}})\ddot{z} - Z_{\dot{z}}\dot{z} - Z_z z - (Z_{\ddot{\theta}}+mX_G)\ddot{\theta} - (Z_{\dot{\theta}}+u_o Z_{\dot{z}})\dot{\theta} - (Z_\theta+u_o Z_{\dot{z}})\theta = Z(ex) \qquad (1)$$

$$(I_y-M_{\ddot{\theta}})\ddot{\theta} - (M_{\dot{\theta}}+u_o M_{\dot{z}})\dot{\theta} - (M_\theta+u_o M_{\dot{z}})\theta - (M_{\ddot{z}}+mX_G)\ddot{z} - M_{\dot{z}}\dot{z} - M_z z = M(ex) \qquad (2)$$

z = displacement in the vertical plane

$\dot{z}$ = velocity in the vertical plane

$\ddot{z}$ = acceleration in the vertical plane

θ = angular displacement in pitch

$\dot{\theta}$ = angular velocity in pitch

$\ddot{\theta}$ = angular acceleration in pitch

u_o = forward velocity of the ship

m = mass of the ship

$Z_{\ddot{z}}$ = added mass coefficient

$Z_{\dot{z}}$ = damping coefficient

Z_z = static restoring force coefficient

X_G = distance from origin to the center of gravity(equal to zero)

$Z_{\ddot{\theta}}$ = coupled virtual mass

$Z_{\dot{\theta}}$ = rotary force derivative coefficient

Z_θ = static force derivative coefficient

I_y = moment of inertia

$M_{\ddot{\theta}}$ = added moment of inertia coefficient

$M_{\dot{\theta}}$ = damping coefficient

M_θ = static restoring moment coefficient

$M_{\dot{z}}$ = coupled virtual moment of inertia coefficient

$M_{\dot{z}}$ = rotary moment derivative coefficient

M_z = static moment derivative coefficient

These equations show a coupling effect between pitch and heave. However, by decoupling these equations and neglecting second order effects, these equations can be reduced to

$$(m - Z_{\ddot{z}})\ddot{z} - Z_{\dot{z}}\dot{z} - Z_z z = Z(ex) \tag{3}$$

$$(I_y - M_{\ddot{\theta}})\ddot{\theta} - M_{\dot{\theta}}\dot{\theta} - M_\theta \theta = M(ex) \tag{4}$$

The equations are now in a form that is readily solvable. The solution of these uncoupled equations is highly significant in determining the motion characteristics of a ship. These characteristics are important in determining stability of motion as well as factors affecting the comfort and safety of personnel embarked on the ship. Before these equations can be solved, however, it is first necessary to determine the hydrodynamic coefficients of added inertia and damping.

The added inertia is a term that results from the fact that a ship moves in a dense medium and therefore must displace a heavy mass of liquid whenever it moves in any plane. This movement of the mass of liquid has the effect of essentially increasing the mass of the ship. The damping is a term associated with energy dissipation and not viscous effects. As a surface ship operates at the interface between water

and air, any vertical motion results in the creation of waves. The energy lost in wave creation acts as a damping force to reduce the oscillations of the ship.

Many methods, both theoretical and experimental, have been developed to determine these coefficients. One such method was developed by Narita (11) at the Massachusetts Institute of Technology in 1962. It consisted of applying a known moment step disturbance to a hull form and measuring the transient response in pitch, while restraining the model from motion in heave. The resultant motion of the model was a transient wave of a decaying sinusoid form leading to the step. When this transient response was obtained, it was used to compute the theoretical response of the model to any known input. This makes use of a property of a linear system, that when its response to a step or impulse input is known, its response to any other input may be found by use of the convolution integral. As a ship is closely approximated by a linear second order system, this principle is applicable.

This property can be used to apply known regular sinusoidal inputs and determine the ship's response. This in essence produces the same results as could be obtained by making forced oscillation tests. The output of the regular sinusoidal inputs can then be used to calculate added mass and damping.

Narita (11) computed added inertia and damping for the pitch motion only. In this work the procedure was extended to measure the coefficients for pitch and heave. Two series of tests were run, one in which the model could pitch with heave restrained and one in which the

model could heave with pitch restrained.

The authors know of no previous tests conducted on the Mariner hull form for the purpose of determining coefficients of damping and added mass. However, a theoretical prediction for the zero-speed condition may be approximated. Porter (14) has reported that the conformal transformation of the unit circle represented by the equation

$$z = \zeta + \sum_{n=0}^{N} a_{2n+1} \zeta^{-(2n+1)} \qquad (5)$$

where z is the plane of the actual ship section and ζ is the plane of the unit circle, can represent a given station of the ship. N is selected and the coefficients a_{2n+1} are found which give the best fit to the actual section. Lewis (10) used this transform with N = 1 and Landweber and Macagno (9) extended it to N = 2. In the present work, a method was used which can give a least mean square error approximation to the actual ship section if the number of coefficients is selected. The least number of coefficients which gave a reasonable fit for each section was used.

After the coefficients of the transform were determined, Porter's method was used to obtain coefficients of damping and added mass for each station at several frequencies and the results were numerically integrated throughout the length of the model by using strip theory to obtain added mass and damping for the model.

CHAPTER II

PROCEDURE

2.1 Model Characteristics

The tests were conducted using a model of the Mariner class hull form, which has the characteristics shown in Table I.

Table I

CHARACTERISTICS OF THE MODEL

Length between perpendiculars	5.28 feet
Beam	.76 feet
Draft	.27 feet
Displacement in fresh water	42.4 pounds
Block coefficient	.6125
Radius of gyration	1.26 feet
Static restoring moment (pitch)	158.84 foot - pounds/radian
Static restoring force (heave)	148.80 pounds/foot
Material of model	Fiberglass, reinforced plastic

2.2 Test Conditions

The tests were conducted at the Massachusetts Institute of Technology ship model towing tank. The tests were divided into two series, pitch with no heave and heave with no pitch. Each series consisted of tests conducted at Froude numbers of 0.0, 0.1, 0.2, 0.3. Further, the tests conducted at zero Froude number were conducted parallel to and perpendicular to the centerline of the towing tank in order to investigate

the effects of wall reflections. In the pitch - no heave, configuration, the ballast weights were shifted in order to determine the effect of changing the radius of gyration on the computed coefficients.

2.3 Step Disturbance Application

2.3.1 General

As the tests were to be conducted in a liquid medium, it was decided that the high potential devices, as recommended by Narita (11), posed a danger to personnel working with the equipment and to other electronic equipment in the event of a wiring mistake or a faulty lead. For this reason low current and voltage devices were investigated, and it was decided that the best device might be a small electromagnet. The magnet chosen for these tests was a simple iron core wound magnet. For the purposes of these tests, the magnet required less than two amperes of current and less than two volts of potential. These values were not only safe to personnel in the event of a casualty, but were easily obtainable with standard direct current power supplies. Initially batteries were employed, but as the tests took a long time, because of delays in waiting for the tank to settle to a dead calm, the batteries rapidly lost their potential. In place of the batteries a Sorenson Model QR 18-1.5A direct current power supply was used.

2.3.2 Pitch - No Heave Configuration

To apply the pitch disturbance, the model was mounted as shown in Figure I. A small metal plate was mounted on the bow and on the stern of the model. A millimeter bar was used to mount the magnet. This

Figure I

PITCH-NO HEAVE CONFIGURATION

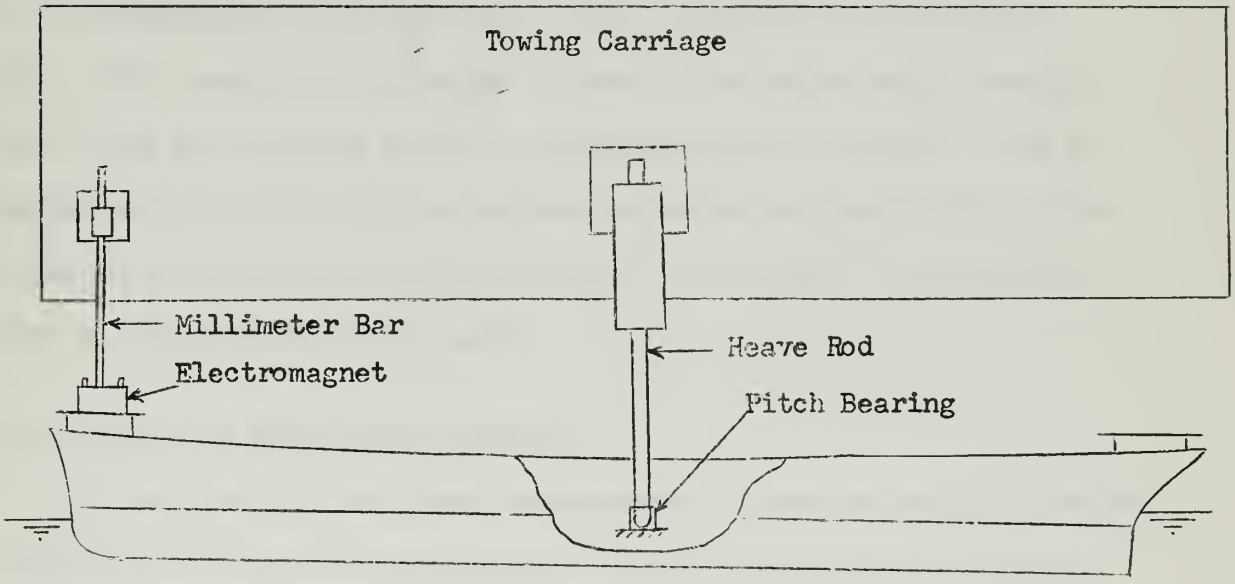

enabled the operators to have greater ease in setting the disturbance at very close to one and a half degrees. As mentioned above, the current was supplied to the magnet from a Sorenson Model QR 18-1.5A direct current power supply. The electric wiring arrangements were as shown in Figure II. By releasing the current to the magnet, the ship will let go under a step-like displacement, following a decaying sinusoid coming to rest at a zero angle of pitch.

As the exact moment is desired at which the ship actually reacts to the disturbance, a second circuit was constructed as shown in Figure III. When the ship begins to react, the magnet parts from the steel plate and produces a step reproduction on the recorder. The beginning point of this step can be used to determine the starting point of the model's response and thus increase the accuracy of calculation based on the response of the model.

2.3.3 Heave - No Pitch Configuration

In constructing the heave arrangements, it was necessary to devise a method of lifting the entire ship. It was also desirable to not introduce any forces tending to cause pitch, which would thus put undue strain on the heave rod. For this reason it was decided to mount a small metal plug directly on the heave rod and to lift the model by connecting the magnet to the metal plug. As the heave rod is mounted approximately at the longitudinal center of floatation of the model, essentially no pitch moment is introduced. The magnet was fastened to the carriage by two aluminum rods as shown in Figure IV. The circuitry is exactly the same as for the pitch configuration.

Figure II

ELECTRIC WIRING ARRANGEMENT

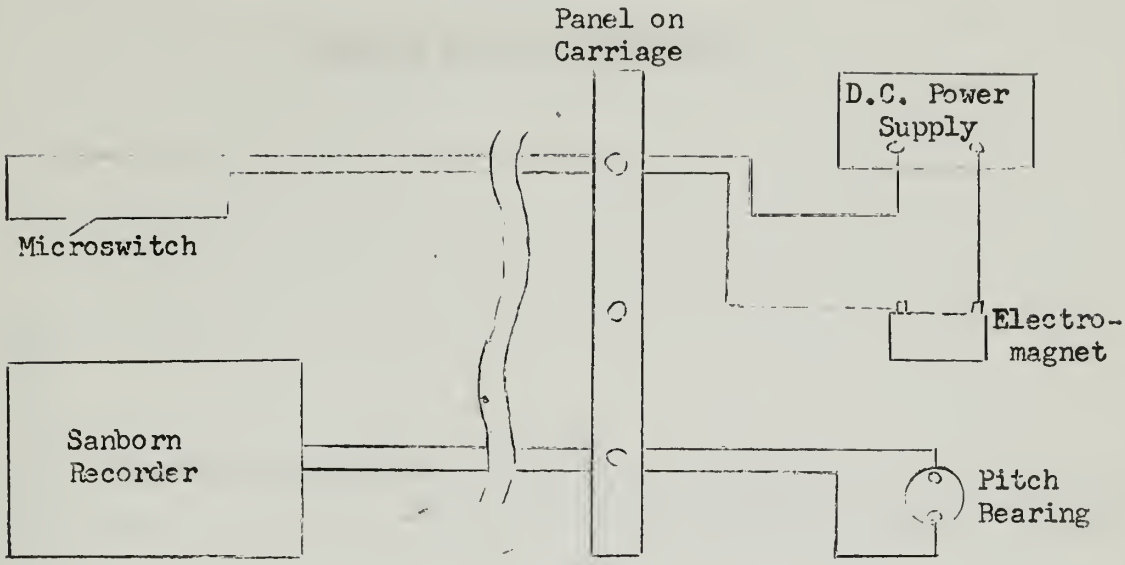

Figure III

MAGNET PARTING CIRCUIT

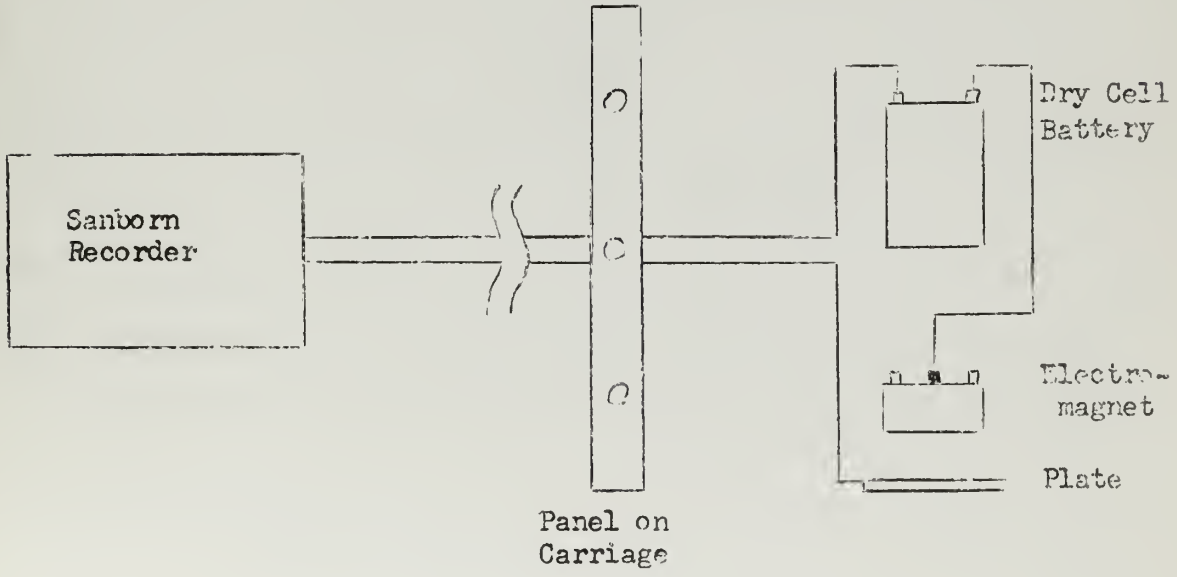

Figure IV

HEAVE-NO PITCH CONFIGURATION

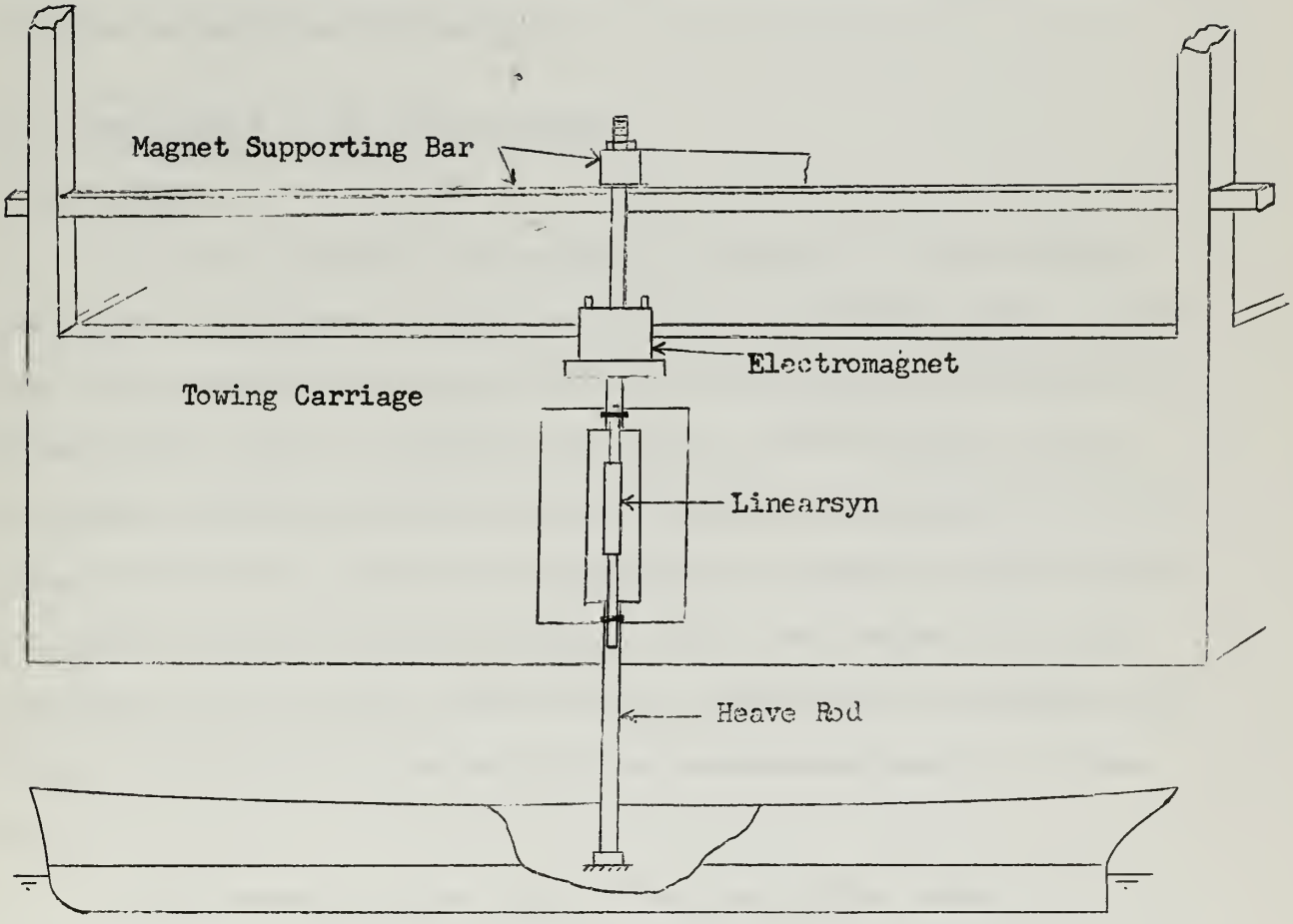

In both heave and pitch testing the magnet and metal connecting plate were mounted rigidly, so there was no concern for catching a falling weight. Then to reconnect, it was only necessary to close the switch and lift the model so that the plate and the magnet came in contact, at which time the magnet would support the weight of the model. Then it was only necessary to wait until the tank settled to an absolute calm before beginning the next run.

2.4 Measurement of the Step Response

2.4.1 Pitch

In order to increase the validity of linearity of motion theory, an initial displacement of only one and a half degrees was used. To get the maximum accuracy in measuring this small variation, two methods were investigated, use of a linearsyn and use of a pitch bearing. To use a linearsyn, maximum excursion of motion is desired. This would be at the ends of the model. However, the motion here is circular enough to cause non-linear motion of the linearsyn and create inaccuracies. Also, the vibrations near the ends of the model were found to be the greatest, and this too would have an adverse effect on measurements made by a linearsyn.

A pitch bearing located right at the longitudinal center of floatation has the advantage that it can measure angular motion right at the point about which pitch takes place. The pitch bearing is a rotary motion displacement pickoff of a differential transformer type and is highly sensitive to any rotary displacement. Therefore, it was decided to employ the pitch bearing for the pitch measurements.

2.4.2 Heave

To measure heave, the linearsyn was perfectly suited. It is a linear motion displacement pickoff of the differential transformer type. It consists of a coil assembly and movable magnetic core and is capable of detecting motions as small as 0.000001 of an inch between the core and coil assembly. Mounted directly onto the heave rod assembly, the linearsyn gives an accurate reading as to the movement of the model in the heave plane.

To increase the validity of model linearity in heave motion, a disturbance of only four-tenths of an inch was applied to the model. This proved sufficient to obtain several well-defined cycles of oscillation.

2.5 Test Procedure

After the model was mounted on the carriage and circuitry arranged, the magnet was connected to either displace the model in pitch or heave, depending on which tests were being conducted. Tests were then carried out in two groups, pitch and heave, at Froude Numbers of 0.0, 0.1, 0.2, 0.3.

With the model displaced it was necessary to wait until the tank had settled to an absolute calm before beginning a test. Then the model was brought up to speed and the switch opened, stopping power to the magnet. At that instant the ship would fall toward zero in a decaying sinusoidal motion, characteristic of a second order system. This motion, as well as the exact instant at which the magnet parted from the metal plate, was recorded on both the Sanborn recording paper and on magnetic

tape for later analysis. To begin the next run, the model had only to be towed back to the opposite end of the tank, the magnet re-engaged with the metal plate, and then allowed to remain suspended until the tank settled.

For the zero speed runs the model was placed at the center of the tank, first parallel to and then perpendicular to the centerline. Here the procedure was the same as before except that there was no forward motion of the model.

CHAPTER III

ANALYSIS

3.1 Background

The analysis procedure used in this work was essentially that used by Kerwin and Narita (5). A step input is applied to a system, and response is represented by

$$P(t) = \frac{1}{C} (1 + R(t)) \tag{6}$$

where C is either the static restoring force in heave or the static restoring moment in pitch. R(t) represents the transient portion of the response and 1/C is the final value the response seeks after the transient has died out.

To get the response to a regular sinusoidal input, the convolution integral is used.

$$V_o(t) = \int_{-\infty}^{\infty} V_i(\tau)\, H(t - \tau)\, d\tau \tag{7}$$

H(t) represents the impulse response of the system. However, as the step response, S(t), is known, it may be used with the input in the form

$$V_o(t) = \int_{-\infty}^{\infty} \frac{dV_i(\tau)}{d\tau} S(t - \tau)\, d\tau \tag{8}$$

and the same results will be obtained. From this, the response of the model to sinusoidal inputs in either heave or pitch may be obtained.

To obtain the damping and virtual mass coefficients, we represent

our second order equations as follows:

$$A_P \frac{d^2\theta}{dt^2} + B_P \frac{d\theta}{dt} + C_P\theta = M_o \sin\omega t \tag{9}$$

$$A_H \frac{d^2z}{dt^2} + B_H \frac{dz}{dt} + C_H z = Z_o \sin\omega t \tag{10}$$

The solution of these equations will be of the form

$$a \sin\omega t + b \cos\omega t \tag{11}$$

from which

$$A_P = \frac{C_P - M_o a_P/(a_P^2 + b_P^2)}{\omega^2} \tag{12}$$

$$B_P = \frac{-M_o b_P}{\omega(a_P^2 + b_P^2)} \tag{13}$$

$$A_H = \frac{C_H - Z_o a_H/(a_H^2 + b_H^2)}{\omega^2} \tag{14}$$

$$B_H = \frac{-Z_o b_H}{\omega(a_H^2 + b_H^2)} \tag{15}$$

3.2 Static Coefficients

Equation (6) indicates that the step response tends to 1/C as the transient dies out. In the initial simplification of the equations, it was assumed that this was a static term and not speed dependent. Gerritsma (2) shows that this term is speed dependent and that this dependency is further a function of the hull form. While the variation in

speed is not great at very low Froude numbers, it does approach approximately 10 percent at a Froude number of three-tenths. This is still not a large effect, but it may exert a measurable influence on the values of added mass and damping calculated at the various Froude numbers.

Accordingly, tests were conducted to determine the change in the static restoring coefficients with speed. In pitch a known moment was applied to the ship and the pitch angle was measured. As the pitch velocity and acceleration were both zero, the static restoring coefficient could be found by dividing the moment by the resultant angle. The static restoring moment at zero speed was computed to be 158.84 ft.-lb./radian. This same procedure was repeated at Froude numbers of 0.1, 0.2, and 0.3, and a variation of less than 1 percent was observed at each speed. Therefore, the static coefficient at zero speed was used for the analysis at each of the Froude numbers.

A known heaving force was then applied to the model, and heave was measured at Froude numbers of 0.0, 0.1, 0.2, 0.3. In this case the results followed the form of those found by Gerritsma as shown in Table II.

Table II

STATIC RESTORING COEFFICIENTS IN HEAVE

Froude Number	Z_z
0	148.8 lbs/ft
.1	141.0 lbs/ft
.2	142.8 lbs/ft
.3	139.2 lbs/ft

The variation is not large, but is significant enough to warrant using the value found at its corresponding Froude number.

3.3 Digitizing Rate

The data as obtained from the experiments was recorded in analog form on magnetic tape. As the convolution integral was performed by series methods, it was necessary to have the data in digital form. Previous experiments conducted by Kerwin and Narita (5) showed the results of added mass and damping to be highly dependent on the digitizing rate used, with damping being the more critical. From their tests of a known second order system, it was found that a digitizing rate of one kilocycle per second gave exact results for added mass and to within three-tenths of 1 per cent for damping.

Accordingly, a digitizing rate of one-thousandth of a second was used. To digitize the data at this rate, it was necessary to record a one kilocycle per second square wave on the tape, as the process used with the IBM 7094 computer reads the value of data everytime there is a positive to negative vertical change in the digitizing signal.

As mentioned earlier, the response of the model was recorded as well as a signal that showed the instant the magnet parted. These signals were recorded first, and the square wave was recorded afterward. The square wave was recorded insuring that it started prior to the instant of the magnet parting signal. By this procedure and obtaining the digitized data for both the response data channel and the parting signal, the parting signal data could be scanned, and the exact instant of magnet parting could be found. On the other channel, this was the starting

point for which the response signal data was used in the analysis program.

As mentioned above, to get maximum accuracy, a digitizing rate of a thousand points per second was used to obtain the best representation of the model response data. In convolving this data with the input sinusoid, a series method was used. This involved shifting the sinusoid in reference to the response data. The response to the sinusoid was computed as a series, and the final value summed. In shifting the waveform, it was found that the fine spacing of .001 seconds was not required. The analysis program was altered to determine what interval could be used and still produce the same results that one-thousandth of a second produced. The main purpose of this alteration was to speed up the analysis program and reduce computer time used in obtaining results. Table III shows the results of increasing the convolution interval at several frequencies or corresponding periods of excitation.

These values were obtained using ideal data for the second order system

$$2.5 \frac{d^2\theta}{dt^2} + 7.5 \frac{d\theta}{dt} + 177\theta \qquad (16)$$

From Table III it can be seen that increasing the convolution interval actually improved the accuracy of results at all except the highest frequency, period equal to 0.64 seconds. In this case the added inertia stayed approximately the same, but the damping became worse by seven-thousandths. The over-all results did show that larger convolution intervals gave accurate results. Accordingly, larger intervals were used

in the analysis, depending on the input excitation frequency.

Table III

EFFECT OF CONVOLUTION INTERVAL ON COEFFICIENTS

Period (Seconds)	Convolution Interval (Seconds)	Added Inertia (Slug Feet^2)	Damping ($\frac{\text{Slug Feet}^2}{\text{Second}}$)
1.28	.001	2.507	7.581
1.28	.010	2.503	7.550
1.28	.010	2.503	7.549
1.28	.020	2.503	7.549
1.28	.032	2.502	7.546
1.28	.040	2.502	7.545
2.56	.001	2.511	7.658
2.56	.010	2.506	7.602
2.56	.016	2.506	7.601
2.56	.020	2.506	7.600
.64	.001	2.498	7.529
.64	.010	2.499	7.536
.64	.020	2.499	7.536

3.4 Theoretical Analysis

In the present problem offsets for 21 stations of the Mariner hull were read off a $\frac{1}{4}$-inch-scale body plan, and by iteration on the IBM 7094 computer, the coefficients a_{2n+1} which gave the best fit to the actual sections were determined. No more than five such coefficients for any one station were used because the physical significance of coefficients beyond a_9 becomes unclear. The values of the coefficients giving the

best fit for each section are tabulated in Table IV.

After the coefficients a_{2n+1} were determined, they were used as inputs to a computer program which utilizes Porter's method as explained in reference 14 and calculates coefficients of damping and added mass for each station. The results for each station were integrated over the length of the model by using strip theory to give the coefficients for the model.

Table IV

SECTION TRANSFORMATION COEFFICIENTS

Station	Half-Beam	Draft	Section Area Coefficient
0	0.20	27.0	7.407
1	4.30	27.0	0.999
2	9.75	27.0	0.818
3	16.15	27.0	0.779
4	22.70	27.0	0.791
5	28.50	27.0	0.830
6	33.25	27.0	0.864
7	36.30	27.0	0.914
8	37.70	27.0	0.958
9	38.00	27.0	0.982
10	38.00	27.0	0.988
11	38.00	27.0	0.979
12	38.00	27.0	0.965
13	38.00	27.0	0.932
14	37.75	27.0	0.868
15	36.45	27.0	0.787
16	33.40	27.0	0.700
17	28.25	27.0	0.609
18	21.05	27.0	0.519
19	12.20	27.0	0.390
20	1.80	0.85	0.020

Table IV (continued)

Station	a_1	a_3	a_5	a_7	a_9
0	-.85755187	-.11659060	-.018916494	+.0065186719	-.00037253164
1	-.660394	-.102210	-.006052	+.021142	
2	-.473941	-.048562	+.012796	+.017246	+.006457
3	-.273985	+.024895	+.024931	+.015372	
4	-.112573	-.017126	+.019732	+.007428	+.007161
5	+.001188	-.032628	+.019083	+.000588	+.005890
6	+.076083	-.053492	+.016873	+.000628	+.005294
7	+.112537	-.078719	+.010882	-.001901	+.001656
8	+.143558	-.103009	+.004784		
9	+.150410	-.118791	-.001681	-.002359	
10	+.150708	-.125100	-.003798	-.002210	+.000777
11	+.151138	-.123101	-.003247	-.003000	
12	+.150843	-.110398	-.001079	-.004638	
13	+.148500	-.085690	+.005438	-.004678	
14	+.140856	-.048439	+.015873	-.004178	+.000558
15	+.124074	-.002855	+.023461	-.001276	+.000786
16	+.081437	+.049610	+.029596	-.001735	
17	-.022515	+.101750	+.042262	-.000402	+.005171
18	-.220882	+.138063	+.078202	+.001977	+.001509
19	-.554295	+.110698	+.101173	+.035004	+.020560
20	+.319277	-.084215	+.054789	-.052018	+.019595

CHAPTER IV

RESULTS

4.1 Heave-No Pitch Condition

To obtain values of added mass and damping in heave, four tests were made at each of the Froude numbers desired. A typical response curve is shown in Appendix B. These curves are presented to show wall reflection effects, but they also show the typical response at zero speed. At forward speeds greater than zero the model response curves were much the same, but considerable vibration was also introduced because of the towing carriage oscillations.

4.1.1 Virtual Mass

The tests conducted at each speed were averaged to obtain the virtual mass. This average value was then nondimensionalized by dividing it by the mass of the model. Each of these values is shown in Table V as a function of excitation frequency. Furthermore, each of the observed values was compared with the average to obtain the worst excursion. This worst excursion from the average is expressed as a percent of the average in Table V.

In most cases all points were very close together, and percentage errors were small. However, occasionally a derived value was at variance with the rest of the results and its error appeared quite large. This took place at those values farthest from the model's natural frequency of approximately 7.6 radians per second.

The symbols used in Table V are as follows:

w radian frequency of excitation

A virtual mass

A' nondimensional added mass

g gravity

Δ displacement of the model

The average values of the virtual mass are plotted in Figure V for each of the four Froude numbers. Figure VI is a comparison of the zero speed values obtained with the model parallel to and perpendicular to the centerline of the tank.

4.1.2 Damping

The same procedure was used with damping as was used with added mass. The results of the average values, as well as the maximum percent error, are shown in Table VI. The damping values were nondimensionalized by multiplying the damping obtained by the square root of the length of the model times gravity divided by the displacement of the model.

Errors in damping were very small, but were generally slightly higher than for added mass. However, near the natural frequency of the model, the errors were very small, increasing as the frequency was increased or decreased.

Additional symbols introduced in Table VI are:

B damping

B' nondimensionalized damping

L length of model

The average values of damping are plotted in Figure VII for each of the four Froude numbers. Figure VIII is a comparison of the zero speed values obtained with the model parallel to and perpendicular to the centerline of the tank.

4.2 Pitch-No Heave Condition

To obtain the values of the added inertia and damping coefficients in pitch, six tests were conducted at each of the Froude numbers. Three tests were conducted with the bow initially up, and three tests were conducted with the stern initially up. The response curves were the same as for the case of heave, in that each was a decaying sinusoid. At speeds other than zero there was a large amount of vibration in the response, paralleling the situation found in heave.

4.2.1 Virtual Inertia

The same analysis program was used to compute the value of virtual inertia in pitch as was used to compute the virtual mass in heave. The only changes were to change several constants and the nondimensionalizing factor. Virtual inertia was nondimensionalized by multiplying the value found by the value of gravity divided by the displacement times the length squared. The values of virtual inertia found at each of the four Froude numbers are shown in Table VII. In this table A designates the value of virtual inertia. Figure IX is a plot of the virtual inertia versus excitation frequency for each of the four Froude numbers. Figure X is a comparison of the zero speed condition with the model parallel to and perpendicular to the centerline of the tank. This figure

also shows the effect on the virtual inertia of changing the radius of gyration of the model from 1.26 feet to 1.17 feet.

4.2.2 Damping

The damping was computed using the same analysis program as for heave with the appropriate constants changed. It was nondimensionalized by multiplying by the square root of the length times the value of gravity and dividing this square root by the displacement times the length squared. The values of damping as a function of Froude number and frequency are shown in Table VIII. The damping is plotted in Figure XI to show its variation with Froude number. Figure XII is a plot of the zero speed conditions, also showing the effect of the reduced radius of gyration.

4.3 Theoretical Results

Based on the coefficients of transformation as presented in Table IV, Porter's theory was applied to determine the coefficients of damping and virtual mass in both pitch and heave. These coefficients were determined at nine frequencies for each station, and the results were numerically integrated by strip theory to obtain the coefficients of virtual mass and damping for the model. These results are presented in Table IX. These same results are plotted in Figures XIII-XVI to compare their values with the experimentally obtained zero speed values.

Table V

VIRTUAL MASS COEFFICIENT IN HEAVE

(1) Froude Number 0.3

w	A	A'	Max. % Error
4.134	1.951	1.481	10.08
4.909	1.741	1.322	8.73
6.042	1.824	1.386	1.04
7.140	1.788	1.358	2.13
7.854	1.752	1.330	1.48
8.727	1.718	1.303	.93
9.817	1.702	1.292	.65
11.220	1.759	1.336	1.42
12.083	1.840	1.398	2.44
13.090	1.891	1.437	3.75

(2) Froude Number 0.2

w	A	A'	Max. % Error
4.134	3.045	2.313	14.86
4.909	2.308	1.751	9.50
6.042	2.129	1.617	8.65
7.140	1.959	1.486	6.48
7.854	1.838	1.395	5.33
8.727	1.732	1.316	4.27
9.817	1.651	1.253	4.18
11.220	1.601	1.217	3.26
12.083	1.625	1.234	7.08
13.090	1.678	1.273	8.11

Table V (continued)

(3) Froude Number 0.1

w	A	A'	Max. % Error
4.134	3.476	2.619	4.21
4.909	2.692	2.041	2.71
6.042	2.282	1.734	7.50
7.140	2.113	1.605	5.35
7.854	1.978	1.501	2.68
8.727	1.845	1.401	3.63
9.817	1.757	1.332	4.10
11.220	1.714	1.301	5.54
12.083	1.754	1.331	5.70
13.090	1.862	1.414	3.44

(4) Froude Number 0.0 (Parallel)

w	A	A'	Max. % Error
4.134	3.876	2.938	.10
4.909	2.845	2.159	1.23
6.042	2.273	1.723	2.86
7.140	2.186	1.659	2.06
7.854	2.054	1.555	1.80
8.727	1.923	1.459	1.35
9.817	1.870	1.418	1.07
11.220	1.905	1.444	.68
12.083	1.879	1.422	.30
13.090	1.993	1.511	.71

Table V (continued)

(5) Froude Number 0.0 (Perpendicular)

w	A	A'	Max. % Error
4.134	2.923	2.220	6.88
4.909	2.696	2.042	7.03
6.042	2.267	1.719	4.10
7.140	2.097	1.590	3.39
7.854	2.030	1.539	4.28
8.727	1.958	1.484	4.75
9.817	1.900	1.440	5.21
11.220	1.901	1.441	6.84
12.083	1.949	1.478	6.57
13.090	2.077	1.572	3.90

Table VI

DAMPING COEFFICIENT IN HEAVE

(1) Froude Number .3

w	B	B'	Max. % Error
4.134	7.333	2.253	3.67
4.909	6.180	1.900	1.38
6.042	5.991	1.841	4.62
7.140	6.494	1.994	2.37
7.854	6.637	2.039	3.92
8.727	6.655	2.045	3.61
9.817	6.420	1.973	3.12
11.220	5.929	1.821	4.00
12.083	6.173	1.897	11.12
13.090	7.295	2.241	9.27

(2) Froude Number .2

w	B	B'	Max. % Error
4.134	4.842	1.488	10.78
4.909	5.279	1.621	15.48
6.042	4.910	1.509	15.32
7.140	5.913	1.828	11.88
7.854	6.213	1.910	7.62
8.727	6.281	1.931	4.00
9.817	6.182	1.901	8.27
11.220	5.636	1.731	46.20
12.083	5.138	1.578	49.70
13.090	4.874	1.499	100.00

Table VI (continued)

(3) Froude Number .1

w	B	B'	Max. % Error
4.134	5.415	1.664	17.67
4.909	7.302	2.245	14.00
6.042	6.429	1.976	7.11
7.140	6.832	2.100	5.14
7.854	7.063	2.172	3.88
8.727	7.045	2.163	1.14
9.817	6.463	1.987	1.89
11.220	5.248	1.612	9.91
12.083	4.305	1.322	16.00
13.090	4.493	1.380	27.21

(4) Froude Number 0 (Parallel)

w	B	B'	Max. % Error
4.134	5.911	1.812	6.96
4.909	8.419	2.582	5.51
6.042	6.660	2.043	2.12
7.140	7.126	2.186	.44
7.854	7.390	2.267	.03
8.727	7.034	2.159	.14
9.817	6.112	1.876	.49
11.220	5.550	1.702	.80
12.083	4.991	1.531	.20
13.090	3.431	1.052	4.20

Table VI (continued)

(5) Froude Number 0 (Perpendicular)

w	B	B'	Max. % Error
4.134	5.325	1.635	10.13
4.909	7.430	2.281	10.52
6.042	8.461	2.600	7.97
7.140	8.304	2.551	1.13
7.854	8.242	2.530	1.72
8.727	8.005	2.458	4.72
9.817	7.279	2.236	10.86
11.220	5.806	1.782	22.10
12.083	4.713	1.448	26.52
13.090	3.773	1.158	45.30

Table VII

VIRTUAL INERTIA COEFFICIENT IN PITCH

(1) Froude Number .3

w	A	A'	Max. % Error
4.134	2.410	.066	7.34
4.909	2.501	.068	6.40
6.042	2.286	.062	3.15
7.140	2.538	.069	1.03
7.854	2.524	.069	1.38
8.727	2.503	.068	1.68
9.817	2.622	.071	3.38
11.220	2.399	.065	3.71
12.083	2.593	.071	4.32
13.090	2.420	.066	6.32

(2) Froude Number .2

w	A	A'	Max. % Error
4.134	2.986	.081	2.11
4.909	2.528	.069	1.42
6.042	2.598	.071	2.38
7.140	2.667	.073	1.35
7.854	2.605	.071	1.11
8.727	2.558	.070	.78
9.817	2.593	.071	.10
11.220	2.434	.066	.70
12.083	2.554	.069	4.67
13.090	2.403	.065	5.86

Table VII (continued)

(3) Froude Number .1

w	A	A'	Max. % Error
4.134	4.020	.109	4.65
4.909	3.538	.096	3.74
6.042	3.019	.082	4.45
7.140	2.715	.074	3.17
7.854	2.551	.069	2.70
8.727	2.412	.066	4.02
9.817	2.316	.063	6.09
11.220	2.200	.060	7.31
12.083	2.150	.058	9.35
13.090	2.181	.059	9.81

(4) Froude Number 0 (Parallel)

w	A	A'	Max. % Error
4.134	3.623	.099	.41
4.909	3.591	.098	.42
6.042	3.167	.086	.36
7.140	2.821	.077	.32
7.854	2.656	.072	.31
8.727	2.519	.068	.24
9.817	2.418	.066	.17
11.220	2.279	.062	.32
12.083	2.199	.060	.10
13.090	2.149	.058	.19

Table VII (continued)

(5) Froude Number 0 (Perpendicular)

W	A	A'	Max. % Error
4.134	1.999	.054	3.10
4.909	3.296	.090	1.40
6.042	3.017	.082	1.28
7.140	2.622	.071	1.37
7.854	2.480	.067	1.59
8.727	2.408	.065	1.74
9.817	2.491	.068	2.69
11.220	2.273	.062	4.53
12.083	2.345	.064	3.67
13.090	2.553	.069	1.61

(6) Froude Number 0 (Reduced R)

W	A	A'	Max. % Error
4.134	3.079	.084	.29
4.909	3.062	.083	.46
6.042	2.674	.073	.10
7.140	2.357	.064	.47
7.854	2.235	.061	.76
8.727	2.134	.058	1.03
9.817	2.074	.056	1.30
11.220	2.037	.055	1.67
12.083	1.998	.054	2.20
13.090	2.049	.056	2.30

Table VIII

DAMPING COEFFICIENT IN PITCH

(1) Froude Number .3

w	B	B'	Max. % Error
4.134	6.651	.073	32.30
4.909	8.514	.094	11.30
6.042	6.157	.068	13.95
7.140	5.887	.065	8.92
7.854	5.876	.065	4.95
8.727	5.155	.057	2.26
9.817	5.130	.057	2.50
11.220	4.343	.048	52.60
12.083	2.021	.022	100.00
13.090	4.762	.052	40.50

(2) Froude Number .2

w	B	B'	Max. % Error
4.134	8.524	.094	4.42
4.909	7.824	.086	2.58
6.042	5.468	.060	6.70
7.140	5.863	.065	3.14
7.854	5.823	.064	.86
8.727	5.189	.057	1.00
9.817	4.981	.055	3.48
11.220	3.588	.043	13.60
12.083	2.921	.032	21.60
13.090	2.003	.022	100.00

Table VIII (continued)

(3) Froude Number 0.1

w	B	B'	Max. % Error
4.134	3.087	.034	14.95
4.909	4.316	.048	1.01
6.042	5.354	.059	1.36
7.140	6.048	.067	2.48
7.854	6.318	.070	1.24
8.727	5.900	.065	3.72
9.817	5.454	.060	5.81
11.220	4.665	.051	9.60
12.083	3.328	.037	13.36
13.090	1.276	.014	20.82

(4) Froude Number 0 (Parallel)

w	B	B'	Max. % Error
4.134	.820	.009	.51
4.909	3.994	.044	1.04
6.042	5.508	.061	.42
7.140	6.173	.068	.53
7.854	6.091	.067	.38
8.727	5.637	.062	.55
9.817	5.102	.056	2.66
11.220	4.205	.046	2.72
12.083	3.155	.035	2.40
13.090	1.491	.016	14.40

Table VIII (continued)

(5) Froude Number 0 (Perpendicular)

w	B	B'	Max. % Error
4.134	-2.723	-.030	1.40
4.909	1.351	.015	14.36
6.042	6.197	.068	2.57
7.140	7.333	.081	1.04
7.854	7.080	.078	.10
8.727	6.353	.070	.88
9.817	5.552	.060	1.15
11.220	7.145	.079	9.64
12.083	3.534	.039	10.83
13.090	10.385	.111	23.60

(6) Froude Number 0 (Reduced R)

w	B	B'	Max. % Error
4.134	1.847	.020	16.83
4.909	3.886	.043	5.90
6.042	6.085	.067	2.26
7.140	6.550	.072	1.43
7.854	6.455	.071	1.25
8.727	6.157	.068	.99
9.817	5.566	.061	.41
11.220	5.395	.059	1.26
12.083	4.701	.052	5.10
13.090	4.578	.050	1.75

Table IX

THEORETICAL VIRTUAL MASS AND DAMPING

Frequency	Virtual Mass	Damping	Virtual Inertia	Damping
4.11	2.823	8.431	4.014	9.605
5.82	2.424	8.540	3.468	10.231
7.13	2.295	7.703	3.230	9.857
8.23	2.257	6.733	3.139	9.272
9.20	2.260	5.933	3.105	8.536
10.08	2.281	5.050	3.073	7.826
10.89	2.310	4.153	3.115	6.378
11.64	2.340	3.893	3.134	6.588
12.80	2.369	3.086	3.157	5.436

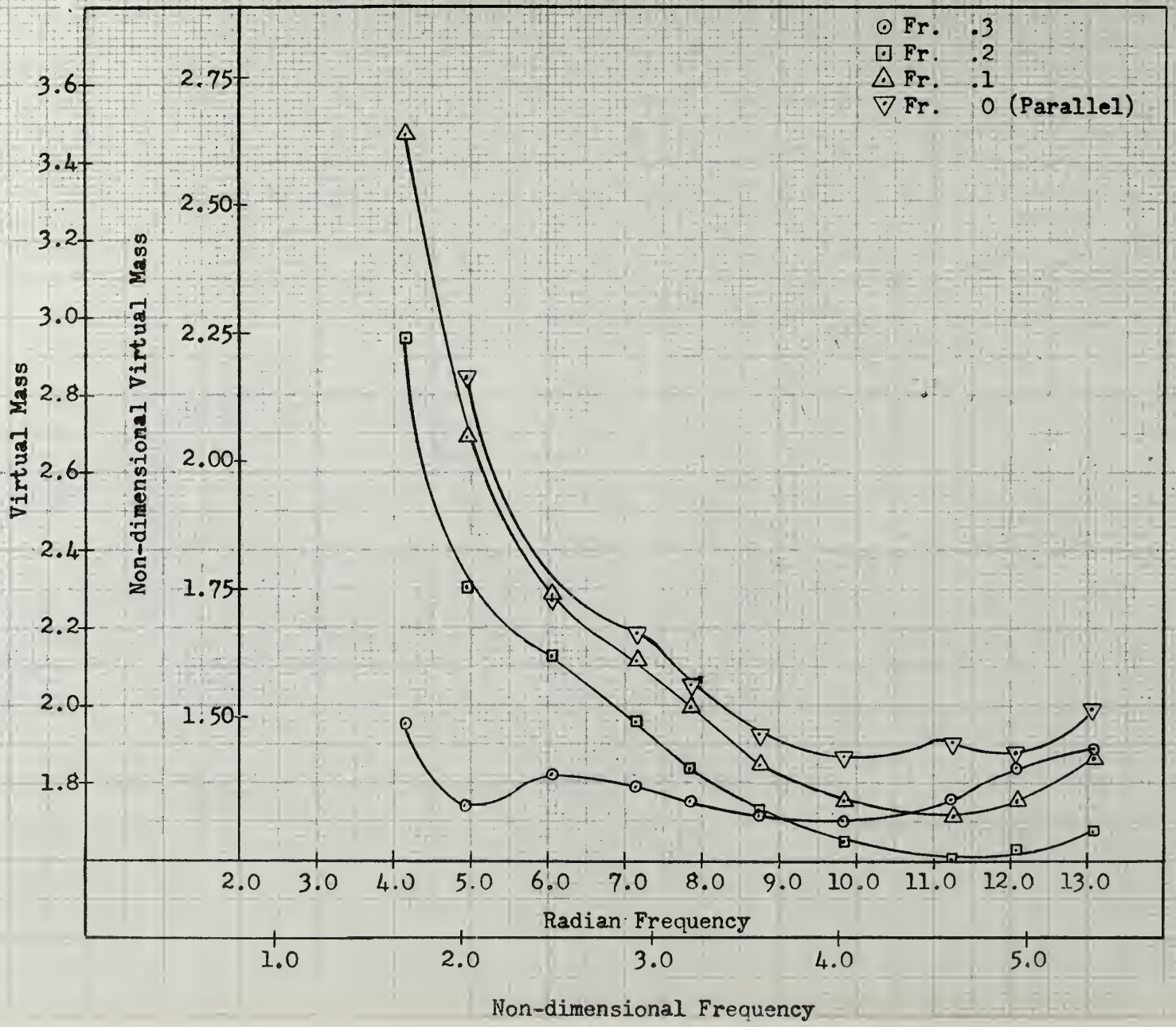

FIGURE V

VIRTUAL MASS IN HEAVE AS A FUNCTION OF FROUDE NUMBER

FIGURE VI

VIRTUAL MASS IN HEAVE AT ZERO FROUDE NUMBER

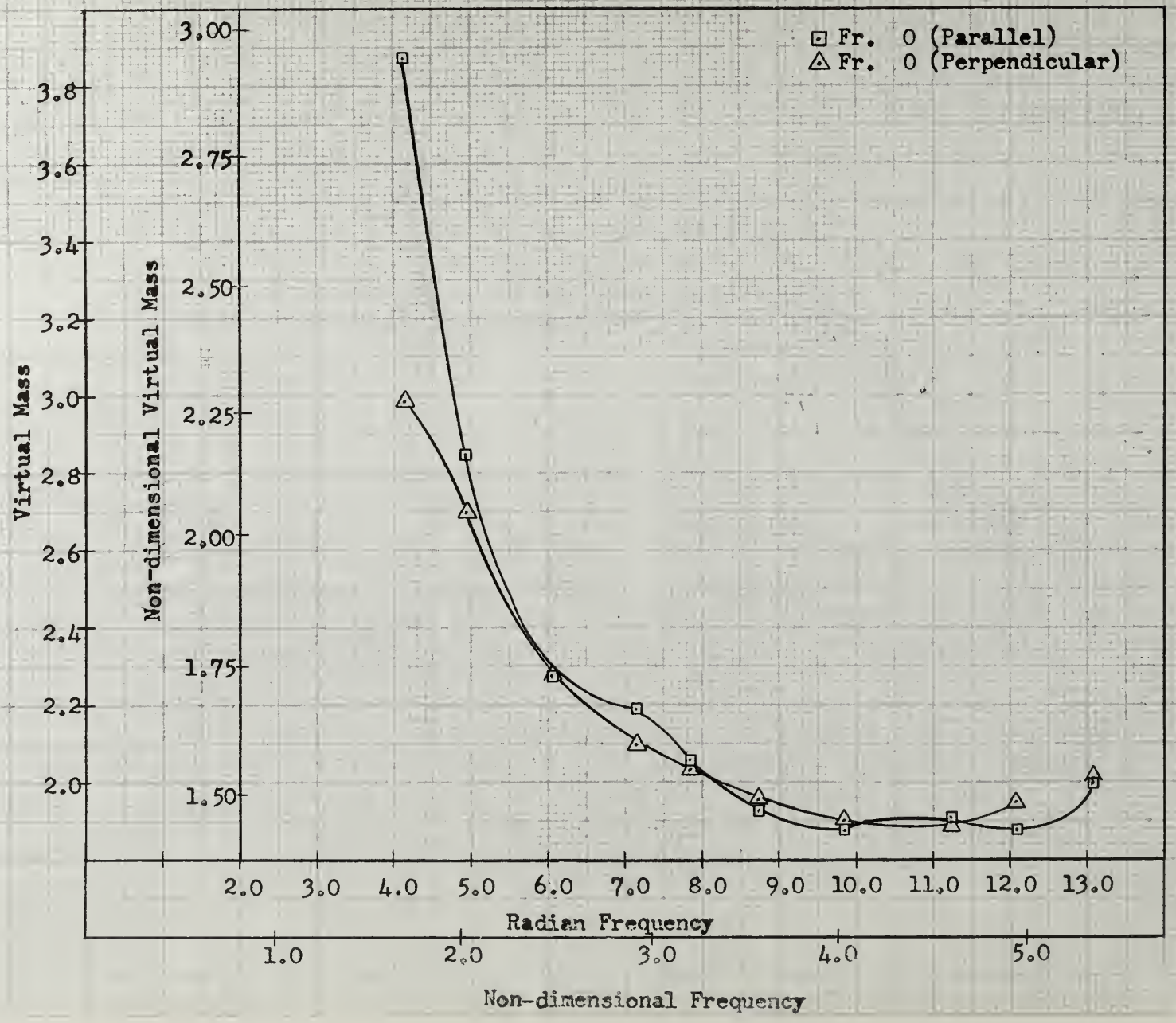

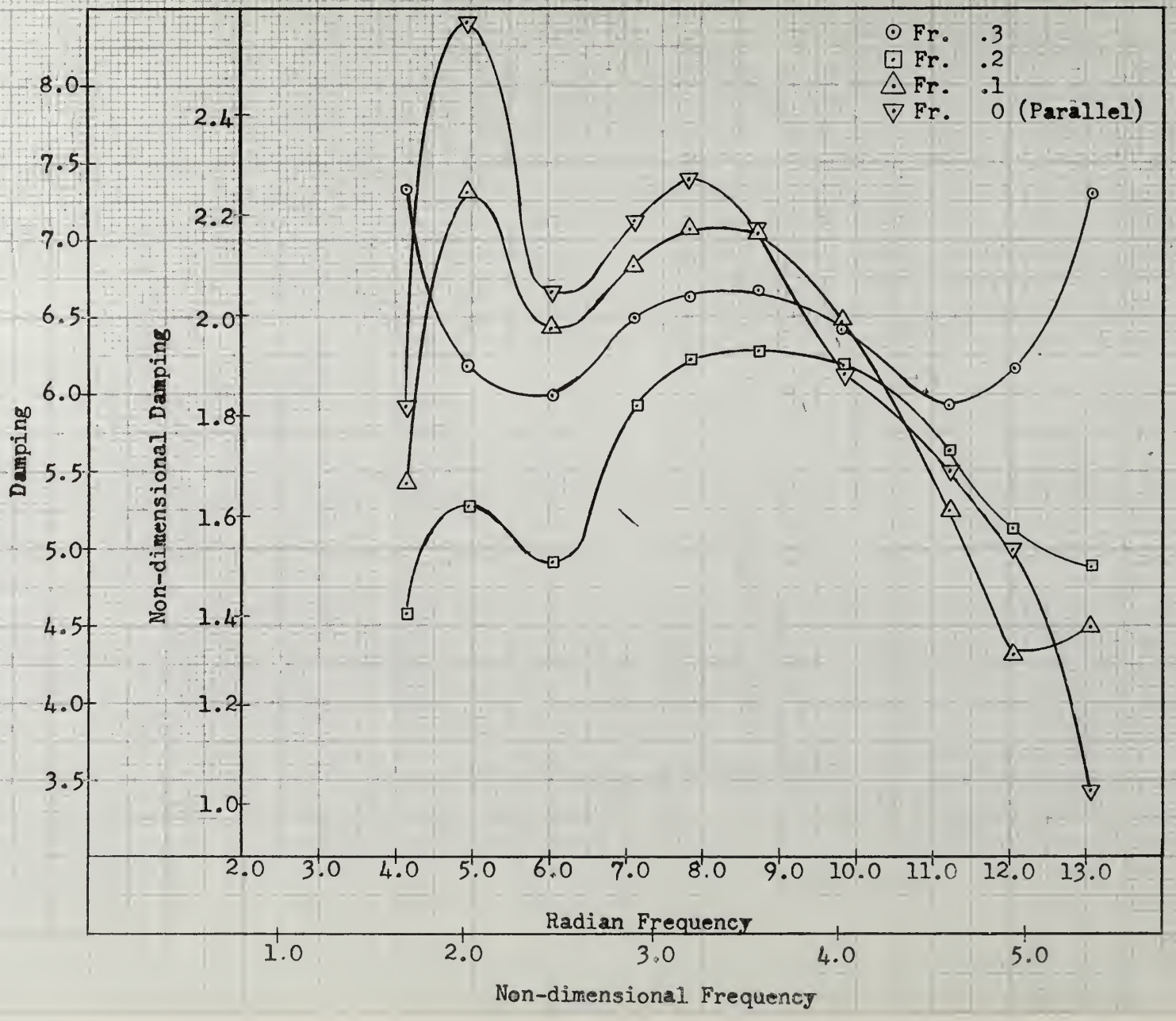

FIGURE VII

DAMPING IN HEAVE AS A FUNCTION OF FROUDE NUMBER

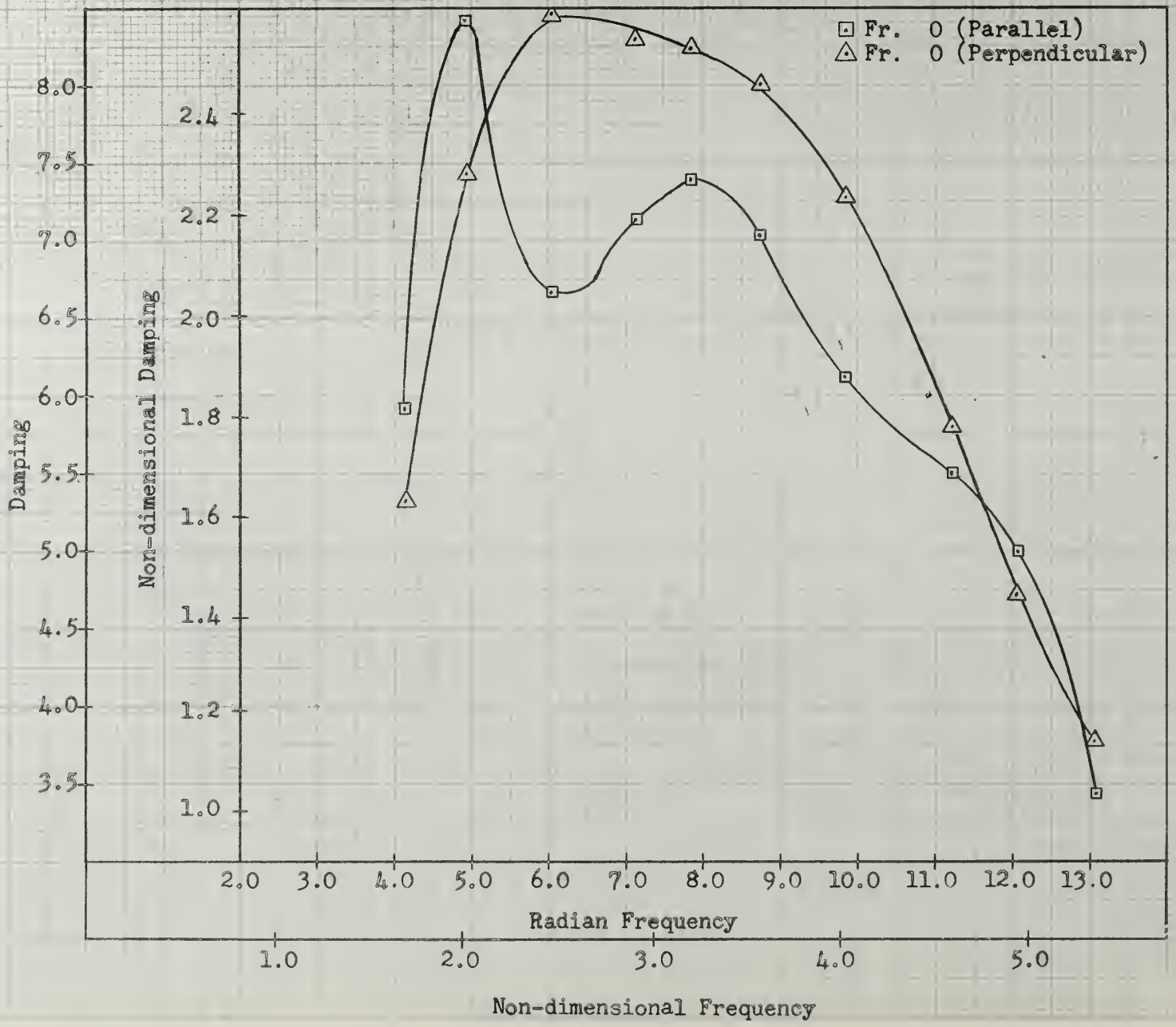

FIGURE VIII

DAMPING IN HEAVE AT ZERO FROUDE NUMBER

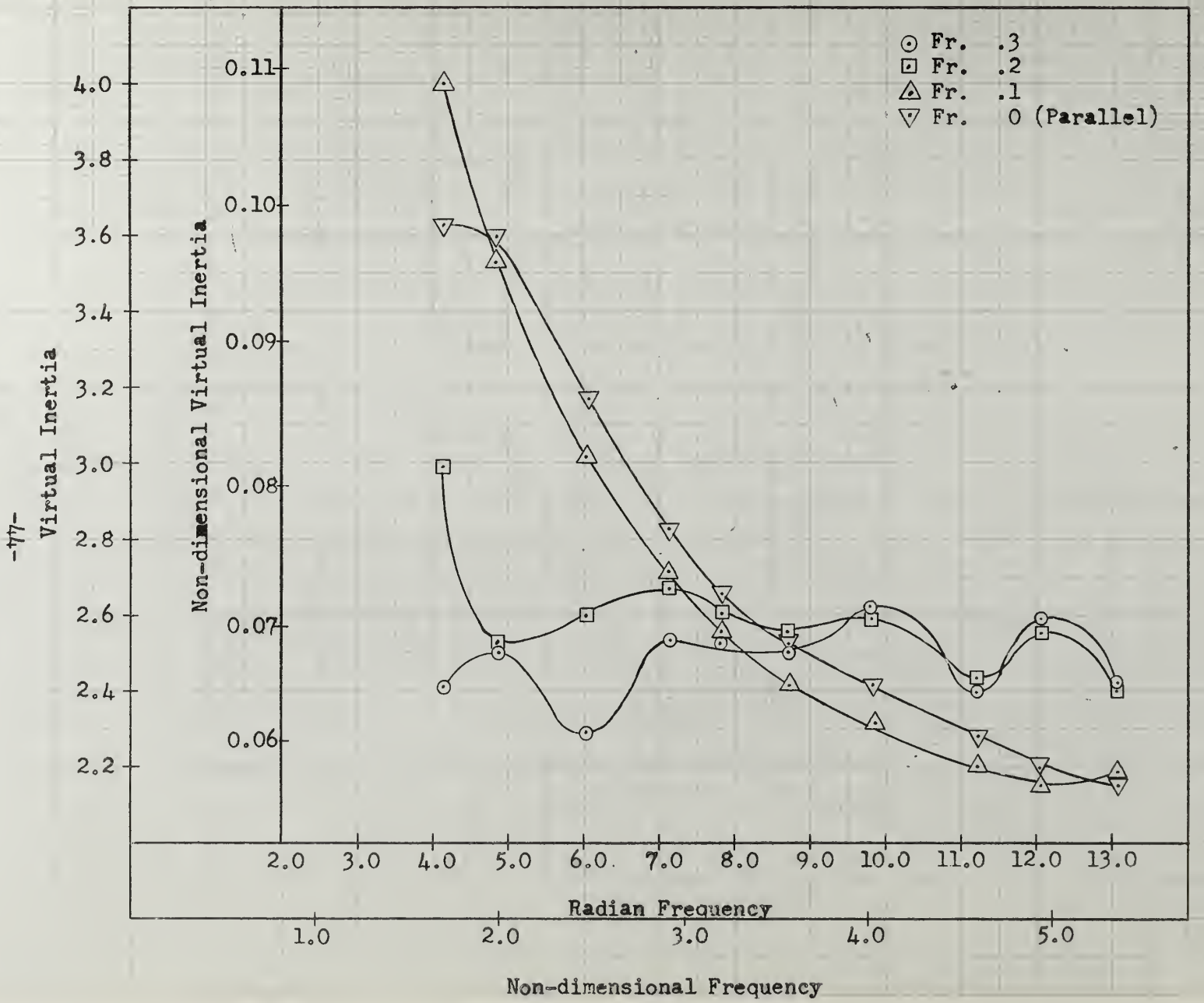

FIGURE IX

VIRTUAL INERTIA IN PITCH AS A FUNCTION OF FROUDE NUMBER

FIGURE X

VIRTUAL INERTIA IN PITCH AT ZERO FROUDE NUMBER

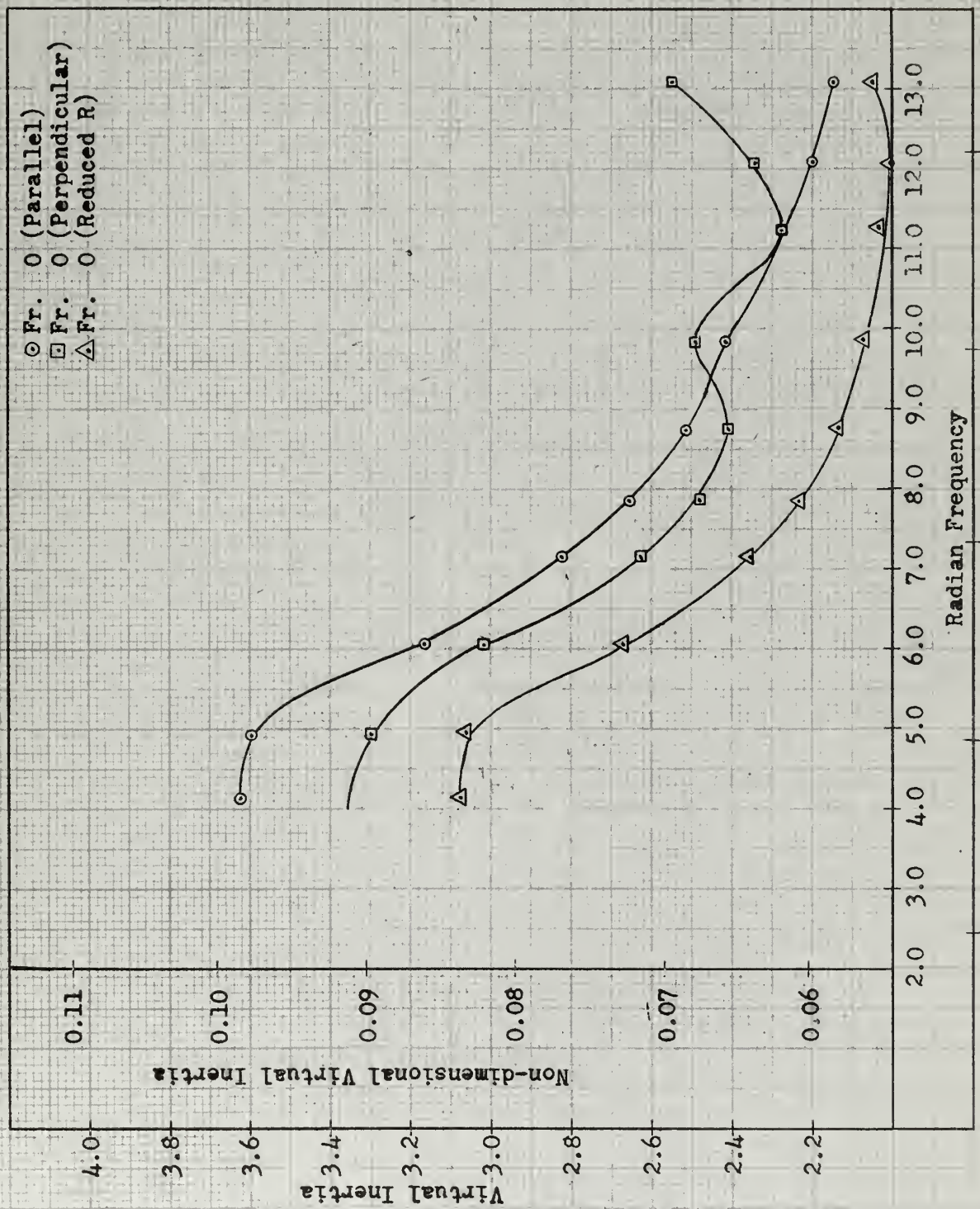

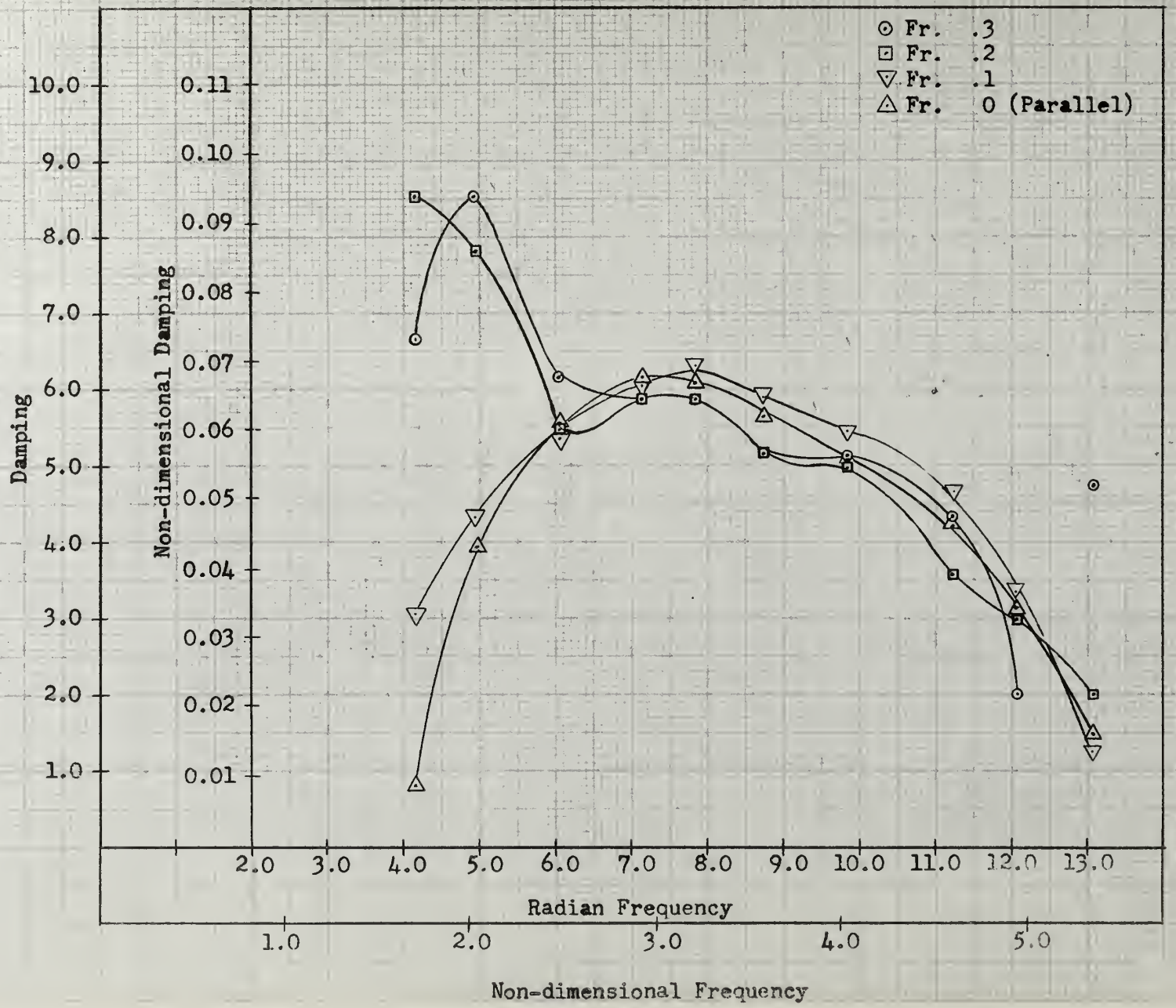

FIGURE XI

DAMPING IN PITCH AS A FUNCTION OF FROUDE NUMBER

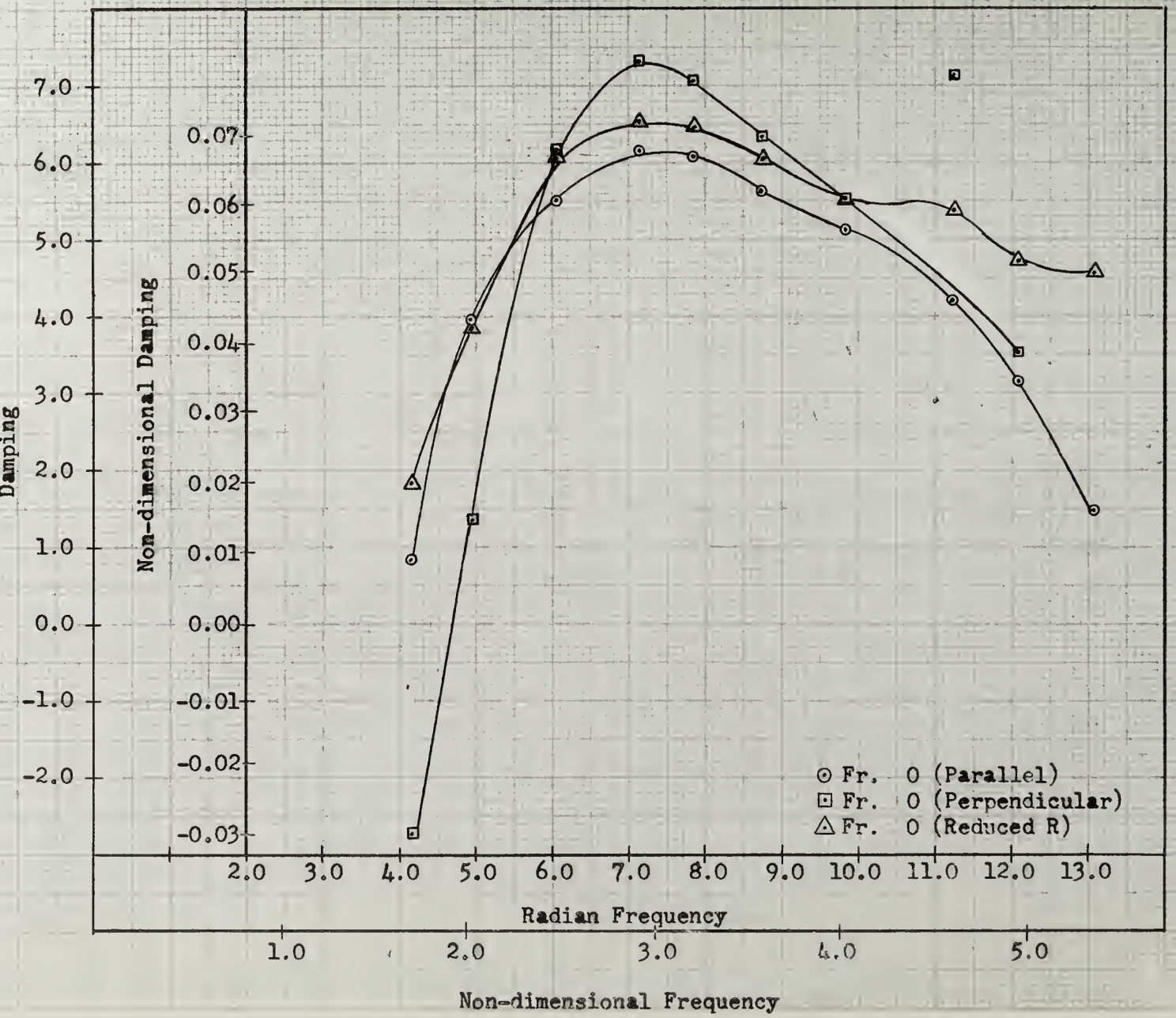

FIGURE XII

DAMPING IN PITCH AT ZERO FROUDE NUMBER

FIGURE XIII

COMPARISON OF THEORETICAL AND EXPERIMENTAL ZERO SPEED VIRTUAL MASS IN HEAVE

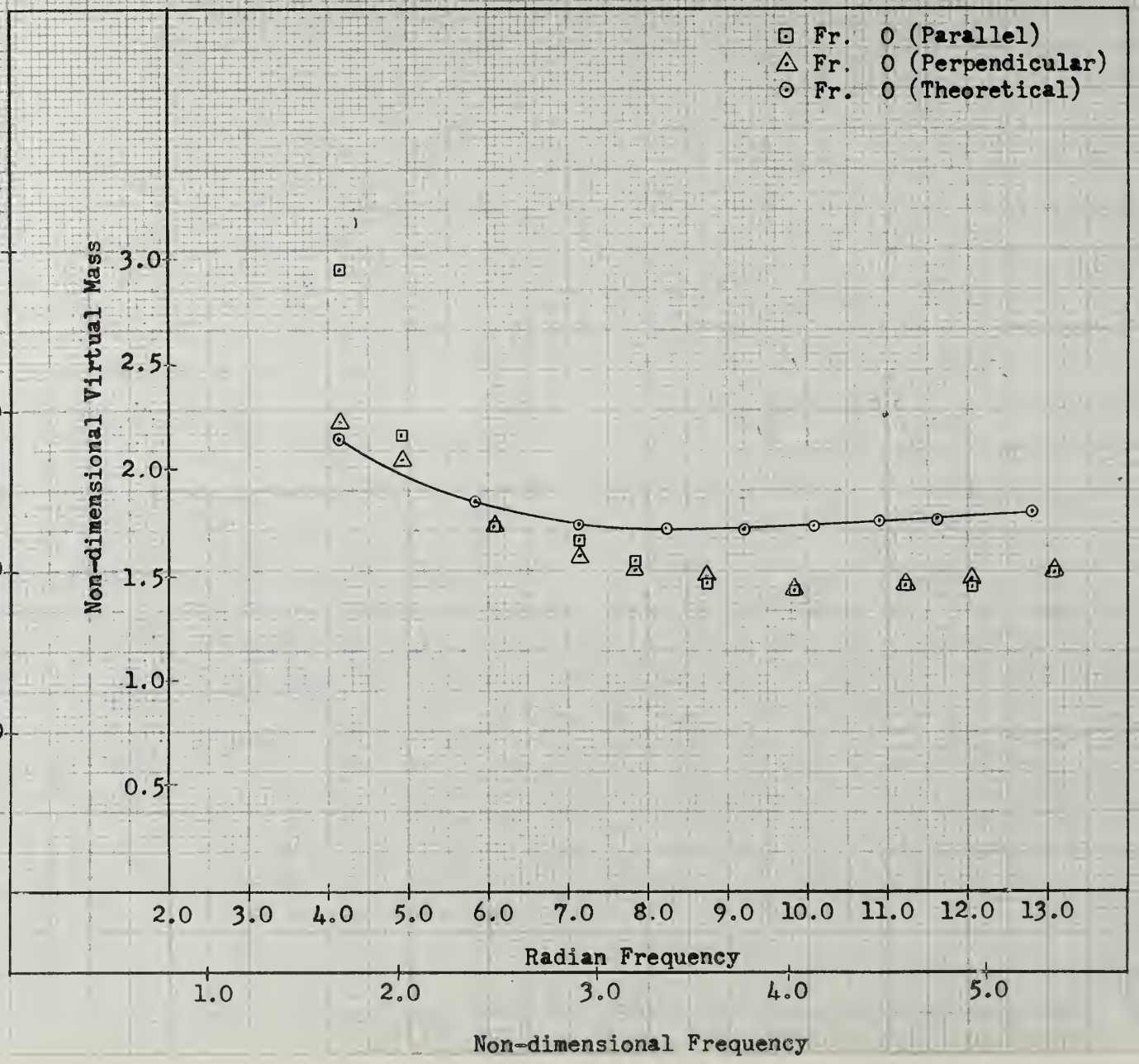

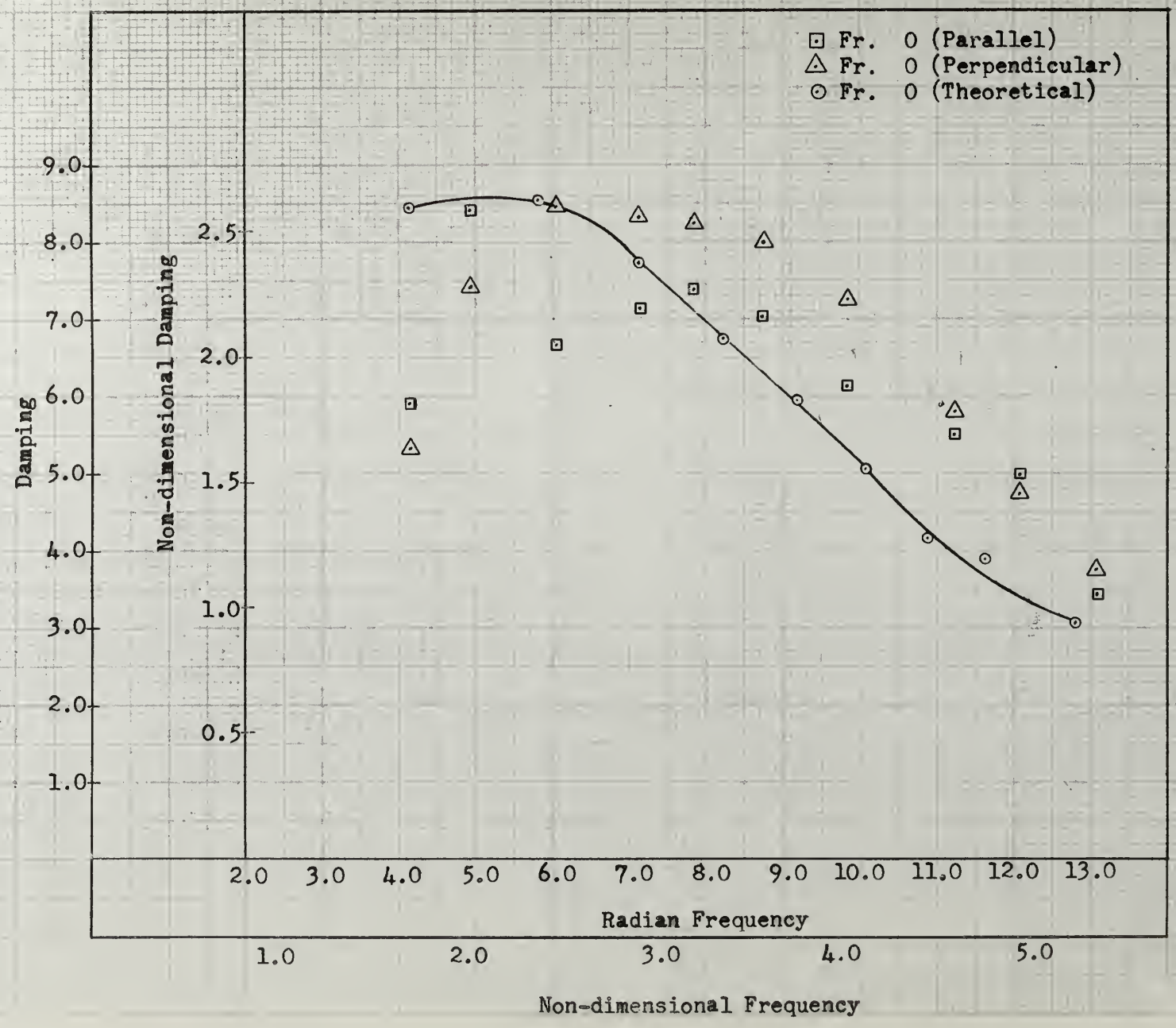

FIGURE XIV

COMPARISON OF THEORETICAL AND EXPERIMENTAL ZERO SPEED DAMPING IN HEAVE

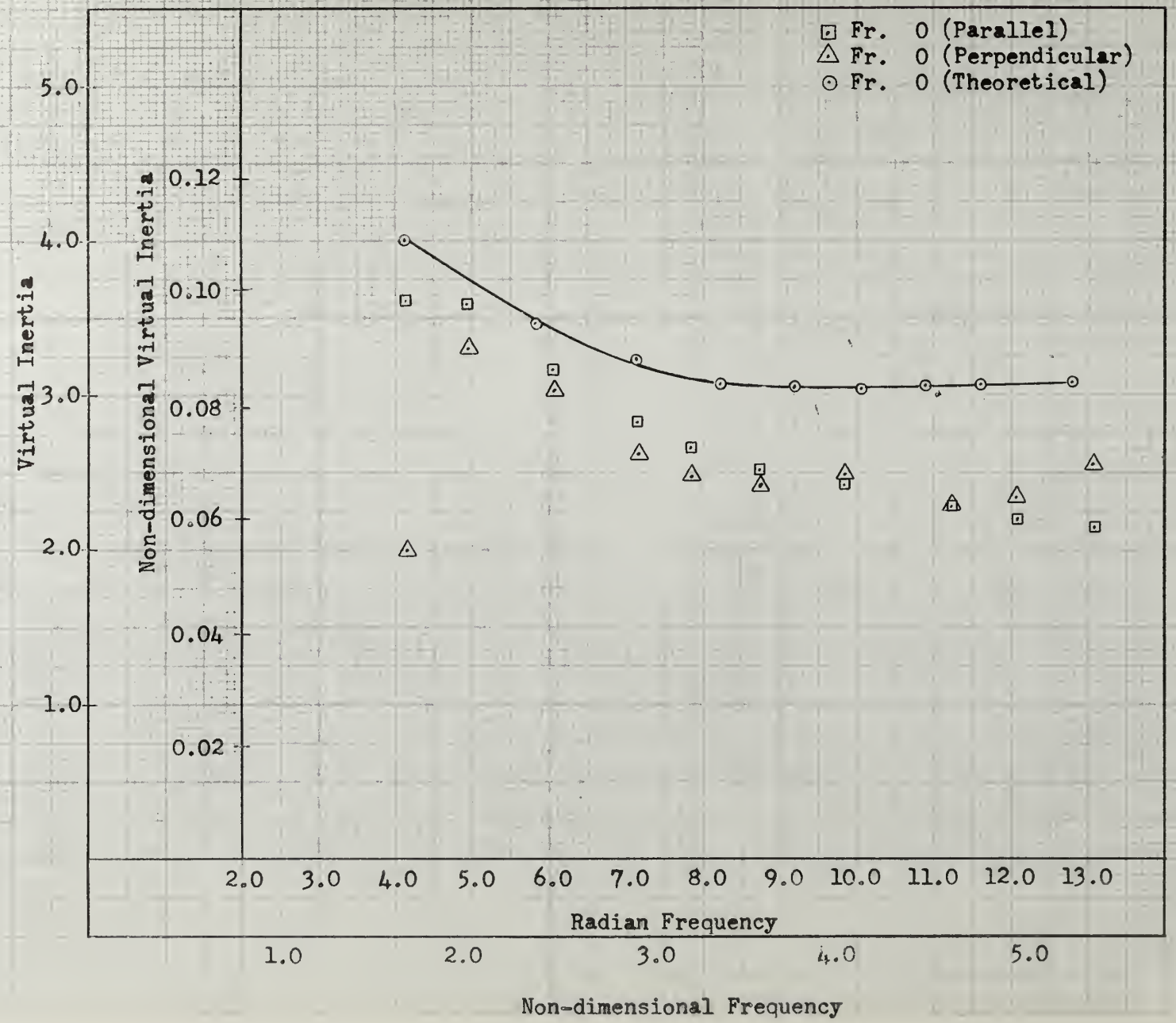

FIGURE XV

COMPARISON OF THEORETICAL AND EXPERIMENTAL ZERO SPEED VIRTUAL INERTIA IN PITCH

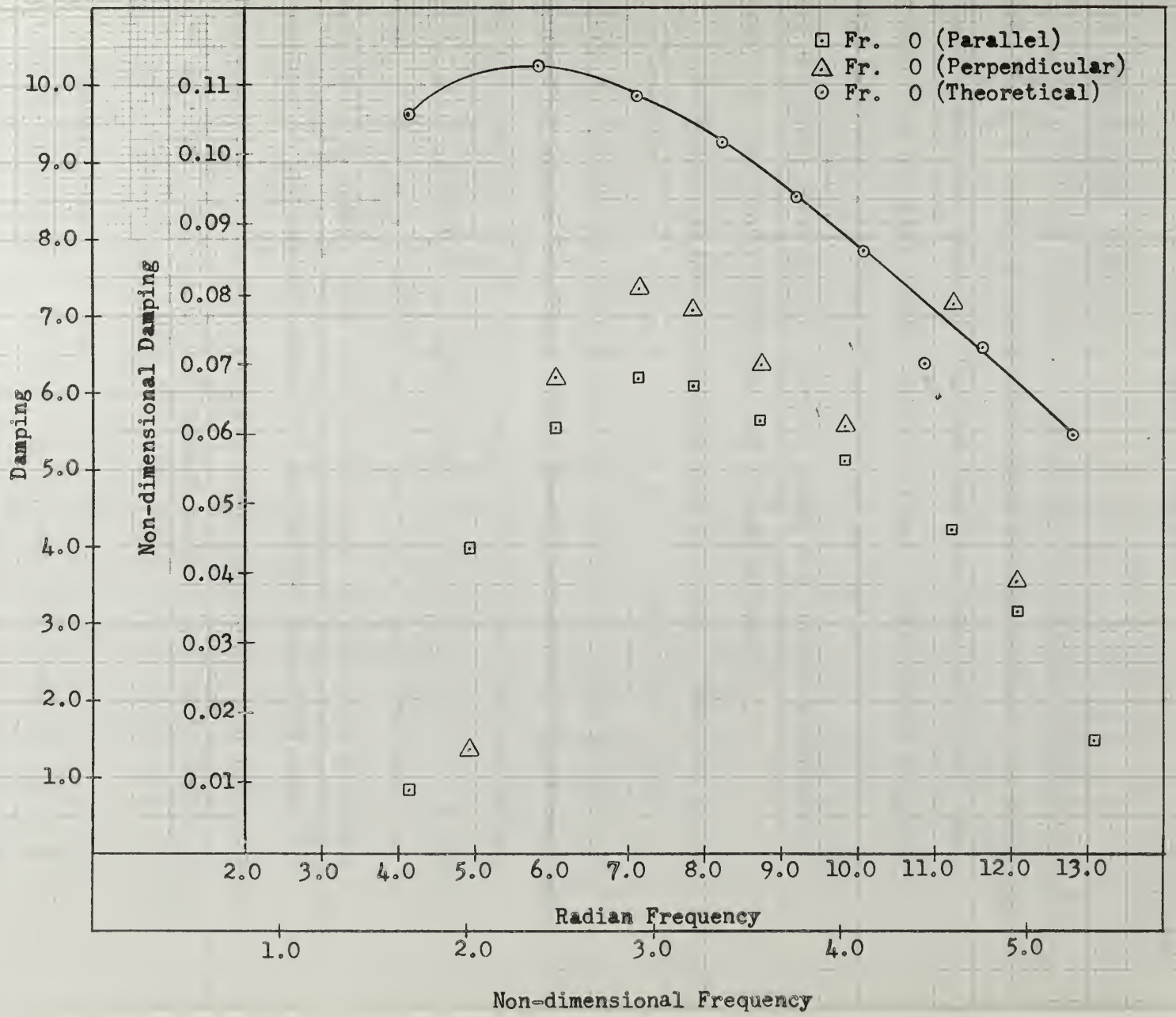

FIGURE XVI

COMPARISON OF THEORETICAL AND EXPERIMENTAL ZERO SPEED DAMPING IN PITCH

Chapter V

DISCUSSION OF RESULTS

5.1 Experimental Errors

The resultant curves of virtual mass and damping as shown in Figures V - XII show the respective values for the Mariner. In comparing these curves with those of other similar type large hullforms, these curves show the same trends in their values. These curves are generally believed to give the values for the Mariner at the various speeds for the given excitations. However, there are several experimental errors or limitations which may limit their accuracy.

Initially the magnet was supported by a wire. When the tests were conducted, the random vibrations were so great as to almost obscure the actual record of the model's motion. For this reason stiff supporting members were used. This greatly reduced the vibrations, but the inherent vibrations in the towing carriage structure and members could not be eliminated. These vibrations became greater at the higher speeds. They were also affected by the rate at which the model was brought up to speed, being much greater when the model was quickly accelerated to the desired speed. In general the vibrations were high frequency with little effect on the results, but since the vibrations were so random, it is likely that there were enough low frequency components to affect the results.

Another source of error was introduced by the procedure used in recording the results. Initially the response was recorded at 3.75 feet per second. At this low speed a one-kilocycle-per-second square

wave would not reproduce on the tape. In transferring the response to a tape at 30 feet per second, it was observed that noise, primarily sixty cycles per second, was picked up. The sixty cycle noise should have had no effect on the results, but any lower frequency components would have. This effect was considered to be very minor.

As mentioned earlier, a second circuit was constructed to record the actual instant at which the model began to drop, as evidenced by the magnet parting from the metal plate. By digitizing this response, it was hoped to be able to pinpoint the proper point on the model response data and not introduce any errors by starting the analysis at the wrong instant. The system was generally satisfactory, but it was sometimes difficult to be sure if the chosen starting point was within two or three thousandths of a second of the actual one. To find the effect of missing the proper starting point, some of the data was analyzed at points away from the initial point. The virtual mass coefficient showed little sensitivity to small changes, while damping tended to be much more dependent on the point at which analysis was begun. Thus, this is a possible cause for the errors being generally larger in damping than in virtual mass.

Because of the use of the rotary pitch bearing, friction was negligible. In heave a definite friction factor was present. However, as discussed in Appendix A , the friction had no effect on the response curve and thus virtually no effect on the final values of virtual mass and damping. To increase the validity of the results, this friction factor should have been included in this analysis program.

5.2 Character of the Results

The resultant curves of virtual mass and damping show the general form as expected. As predicted by Grim, the curves of virtual mass should drop sharply from infinity to a minimum and then rise to an asymptotic value. The infinite point should occur at approximately a radian frequency of $\frac{\omega u_o}{g} = \frac{1}{4}$. While the range of frequencies investigated do not show this point, they do definitely show this trend as it is seen that the curves tend toward infinity at frequencies inversely proportional to speed, the higher speeds rising at lower frequencies.

The values of damping also showed the same trend as for other ships. Theory predicts that damping should go to zero at higher frequencies. However, experimental techniques have shown damping to rise at higher frequencies. This indicates that the theory is only good at low frequencies. In some cases the damping appeared to still be falling to zero in these experiments. However, the higher speeds showed a definite rise. The lower speeds were not tested at higher frequencies, as this is the general region of towing carriage equipment natural frequencies. In this region the validity of the results was somewhat questionable anyway.

For the curves in general a study of the results shows the agreement of the results in the vicinity of the natural frequency of the model to be very good. At frequencies removed from this value the errors went up considerably. This indicated that this method is accurate only near the model's natural frequency. Also, as mentioned earlier, the errors in virtual mass were much less than for damping, indicating

that the procedure may be better for determination of added mass than for damping. At the higher frequencies this effect became very pronounced but was also affected by equipment natural frequencies.

Kerwin and Narita noted a sudden drop in damping at approximately eleven radians per second. This was attributed to the natural frequency of the heave rod. In this series of tests a much stiffer heave rod was used in an effort to extend the range of frequencies. This sharp dip appears to have been eliminated, but there is enough fluctuation at frequencies above eleven radians per second to render these results of little value. Thus this indicates an even stiffer heave rod would be desirable.

To overcome the problem of frequency range limitations, there is also the possibility of altering the model's natural frequency. This was investigated by changing the position of the ballast weights to change the radius of gyration. In analyzing the effect of this alteration, the damping did not appear to change but fell somewhat between the two other zero speed conditions. The virtual inertia did change as expected and is shown in Figure X.

The results obtained in pitch did not depend on whether the model was initially bow up or stern up. In heave the results were all obtained with the model lifted up. If a method were used to put pressure on the model in order to start with it initially down in the water, it would probably produce the same results as when it started lifted up. This supports the principle of linearity which was assumed in this entire procedure.

5.3 Theoretical Results

5.3.1 Transformation Coefficients

The values of the transformation coefficients a_{2n+1} were found which mapped a cylinder into the sections of the Mariner. The agreement between the mapped sections and the actual sections was very good in the vicinity of amidships, while the greatest excursions were near the ends. For example, at station nine the maximum difference between the mapped section and the actual section was only 0.08 feet with an average excursion of 0.039 feet. The worst fit occured at station one, which had a maximum excursion of 0.9315 feet and an average excursion of 0.422 feet. The average excursion for the entire ship was 0.168 feet. A plot showing the difference in the mapped and actual form at station one is given in Appendix C.

5.3.2 Comparison of Theoretical and Experimental Results

From Figures XIII and XIV one can see that the theoretical values of virtual mass and damping in heave compare quite favorably with the experimentally derived values. The virtual mass values show closer agreement than do the damping values. However, the difference between the theoretical and experimental damping is of the same order as in the two experimental values found from essentially identical response curves. This shows the extreme sensitivity of damping to any minor differences, and perhaps strip theory is not a precise enough method to evaluate damping, unless very fine station spacing were used.

In pitch the agreement between the experimental and theoretical values of virtual inertia was better than the agreement in damping.

However, in both cases the variations were greater than for the corresponding values in heave. This variation was believed to be the result of using strip theory on the Mariner hullform. The Mariner has a bulbous bow and a wide flared stern. These sections produced a comparatively large value for both added mass and damping. To use strip theory in pitch, each section is multiplied by the distance from the center of gravity squared and then integrated over the length of the model. These extreme bow and stern sections had a very large arm to the center of gravity and thus produced very great factors. In the actual case there are two reasons why the strip theory is questioned. Near the bow and stern the flow is not two-dimensional, as it is near amidship, and thus the use of strip theory is not as valid. For example, near the ends the water can vent itself not only at the sides, but also at the ends, which should reduce the values found there. These factors may have caused the theoretical values to be higher than the values found experimentally.

As in heave, it is believed that much finer spacing of sections should be used, especially near the bow and stern in order to obtain better results for the theoretical values. This will not correct the error resulting from three dimensional effects, but would reduce errors caused by too large an integrating interval in the vicinity of these critical regions.

Chapter VI

CONCLUSIONS

6.1 Evaluation of Step Method

It is considered from the results of this work that the step disturbance method is a good method for obtaining added mass and damping coefficients. It has several advantages in that the experiment is very easy to set up. By use of a device, such as a magnet, it requires only low potential devices for power requirements, which are readily available. The calculations involved would be virtually impossible if done by hand, but they are readily adaptable to computer operation. One problem that may arise with some models is the problem of wall reflections in a narrow tank. This was not a factor in the Mariner tests, but by orienting the model to the centerline of the tank at various angles, this problem can be overcome.

It is concluded further that the process is better suited for added mass than for damping. This is a factor of the experiment and the analysis program. Damping variations were much greater because of vibrations or not having the exact starting point in the data. From the analysis program, it was seen even with exact generated data, damping showed variation from the actual values. However, if care is taken to get minimum vibrations and if the data is sampled at fine enough intervals, it is believed that the process is valid for damping as well as for added mass.

A limiting feature of the experiment is the dependence of the results on the model's natural frequency. This, coupled with the

interference of the supporting structure's natural frequency, could limit the range of reliable results. By using a very stiff heave rod and bracing it, its natural frequency could be made high enough to not interfere with the results.

6.2 Experimental Results

It is observed from the experiments that both added mass and damping are speed dependent. However, in the vicinity of the natural frequency of the model, this dependency is very slight. The speed dependence was generally greatest at the lower frequencies.

Virtual mass was affected by the model's natural frequency, while damping showed little dependence. Thus it appears possible to extend the useful range of frequencies in damping by testing the model at various natural frequencies. For virtual mass calculations the proper natural frequency desired must be used for the model.

6.3 Theoretical Conclusions

The method of mapping a cylinder into a ship section is very good if sufficient coefficients are used. With the exception of highly irregular sections, almost perfect agreement between mapped and actual sections can be obtained. However, the extent of the calculations make it almost impossible to perform them by hand, but they are readily adaptable to computer operation.

The virtual mass and damping coefficients derived from this method were believed to be accurate, as evidenced by the results obtained in heave. However, to apply strip theory to the results in pitch, it is

recommended that finer spacing be used at the bow and stern, especially for irregular sections such as are on the Mariner. By this method a more accurate representation of the virtual inertia and damping coefficients at the ends of the model could be obtained. Thus, when multiplied by the distance to the center of gravity squared, these sections would probably not produce the effect of having the bow and stern dominate in obtaining the coefficients of virtual inertia and damping for the model.

Chapter VII

RECOMMENDATIONS

7.1 Experimental Technique

The major problem faced in analyzing the data was obtaining the data in digital form. The analog to digital program used was very efficient, but there were several mistakes made by the operators which, if not made, would have greatly aided the obtaining of the digital output.

The first problem was recording data at too slow a speed and not being able to record the digitizing signal. The tape recorder has to run at a speed of thirty feet per second to record a one-kilocycle-per-second square wave properly.

Each run took approximately twenty-two seconds to digitize. If data were recorded with this spacing between runs, the digitizing console should be set up to run continuously, and there would be no lost time in setting the start of each run when the computer was ready for more data.

In setting up the digitizing console, one has to set up an amplifying and an offset section so as to keep the data between plus and minus eight volts. It is best to get as wide a spread as possible in order to get the maximum resolution of the data. In order to get this spread and not have any data be clipped, it is essential that all runs be recorded to the same scale. Thus in setting up the recording equipment, the zero position and maximum deflection position should be made the same on the recording equipment for every run. Otherwise reduced

scales must be used to keep all data within the allowable range, with some loss in accuracy.

The final point to be made about digitizing concerns the treatment of the magnet parting signal. The method employed by the operators in this instance produced several problems that could have been avoided. The first problem was that in putting the one kilocycle square wave on the tape, the instant of magnet parting was missed in some cases as the square wave was put on the tape too late. These runs had to be digitized a second time to get useful data. This was a waste of computer time that was necessary to get the maximum amount of data analyzed. Finally, in scanning the record of the parting signal, it is possible that the starting point may have been missed by a couple thousandths of a second. This same accuracy could have been obtained by simpler methods. The best method appears to be to wire the square wave generator between the recorder and the magnet such that when the magnet parts, the square wave begins recording. This process should have negligible time delay.

The other big problem was that of random vibrations in the data. As stiff a supporting member as possible should be used for supporting the ship and supporting the magnet. This would not only reduce the vibrations, but also would not limit results because of the equipment's natural frequency. Also, the model should be accelerated up to speed as slowly as possible to minimize the vibrations caused by this acceleration.

To increase the validity of the results found in heave, a device

employing rotary joints and stiff members may have the benefit of less friction than the heave rod. The inertia of the mechanism may be difficult to determine, but it may be a better mechanism for this type of experiment.

7.2 Future Studies

The method employed here is considered a good one and could be applied to further studies in ship motions. It could possibly be used to obtain the values of the coupling coefficients between pitch and heave. This could be done with a similar arrangement in which the model were allowed both types of freedom, and the two motions recorded. The method could also be extended to further studies of damping. This could be done by measuring the relation between wave amplitude at the side and the amplitude of the model's oscillation in heave. The same linearity assumptions could be employed, and the results compared with those obtained by forced oscillation tests.

BIBLIOGRAPHY

1. Abkowitz, M. A., "The Linearized Equations of Motion for the Pitching and Heaving of Ships," Proceedings, Symposium on the Behavior of Ships in a Seaway, Netherlands Ship Model Basin, Wageningen, 1957, pp. 178-189.

2. Gerritsma, J., "Shipmotions in Longitudinal Waves," International Shipbuilding Progress, Vol. 7, No. 66, February, 1960, pp. 49-76.

3. Golovato, P., "The Forces and Moments on a Heaving Surface Ship," Journal of Ship Research, Vol. 1, No. 1, April, 1957, pp. 19-26.

4. Grim, O., "A Method for a More Precise Computation of Heaving and Pitching Motions in Both Smooth Water and in Waves," Proceedings of Third Symposium on Naval Hydrodynamics, Office of Naval Research, Department of the Navy, ACR-55, 1960.

5. Kerwin, J. E. and H. Narita , "Determination of Ship Motion Parameters by a Step Response Technique," M.I.T., Department of Naval Architecture and Marine Engineering, (to be published).

6. Korvin-Kroukovsky, B. V., Theory of Seakeeping, New York: Society of Naval Architects and Marine Engineers, 1959.

7. Korvin-Kroukovsky, B. V., "Brief Review of Ship Damping in Heaving and Pitching Oscillations," Stevens Institute of Technology, February, 1955.

8. Landweber, L. and Matilde Macagno, "Added Mass of Two-Dimensional Forms Oscillating in a Free Surface," Journal of Ship Research, Vol. 1, 1957.

9. Landweber, L. and Matilde Macagno, "Added Mass of a Three-Parameter Family of Two-Dimensional Forces Oscillating in a Free Surface," Journal of Ship Research, Vol. 2, 1959.

10. Lewis, F. M., "The Inertia of the Water Surrounding a Vibrating Ship," Transactions of the Society of Naval Architects and Marine Engineers, Vol. 37, 1929.

11. Narita, H., "A Step Response Analysis of Damping and Virtual Inertia of a Pitching Ship Model," M.I.T., Department of Naval Architecture and Marine Engineering, May, 1962.

12. Newman, J. N., "The Damping and Wave Resistance of a Pitching and Heaving Ship," Journal of Ship Research, Vol. 3, No. 1, June, 1959, pp. 1-19.

13. Newman, J. N., "On the Damping of Pitch and Heave," Journal of Ship Research, Vol. 1, No. 2, July, 1957, pp. 48-53.

14. Paulling, J. R. and W. R. Porter, "Analysis and Measurement of Pressure and Forces on Heaving Cylinders in a Free Surface," Proceedings of the Fourth U. S. National Congress of Applied Mechanics, 1962.

15. Vassilopoulos, L. and P. Mandel, "A New Appraisal of Strip Theory," M.I.T., Department of Naval Architecture and Marine Engineering, August, 1964.

16. "Nomenclature for Treating the Motions of a Submerged Body Through a Fluid," Bulletin No. 1-5, The Society of Naval Architects and Marine Engineers.

APPENDIX

APPENDIX A

DISCUSSION OF EQUIPMENT FRICTION

In choosing the components of the towing apparatus that allowed pitch and heave motions of the ship, and in choosing the measuring devices, it was desired to eliminate or reduce friction to a minimum. Before any connection or measuring plans were made, this was the first consideration.

The problem in pitch was not very great. The only moving connection, which also contained the measuring device, was the pitch bearing. It is a small bearing rotary device and contributed no noticeable friction.

In heave the problem was much greater. The first idea was a mechanism employing straight bars connected by small bearing pivots. While there would be several such pivots, each would have essentially no friction, and the net effect would approach frictionless operation. The biggest problem was the system complexity required to insure heave motion only. Also, there was a problem of determining the exact system inertia in motion.

Because of the above problems, it was decided to investigate the use of a heave rod. Previous heave rods employed had a large amount of friction. A new one was constructed using a square rod moving on a system of small roller bearings. Friction tests were conducted on it by a weight-dropping method. Various weights were attached to the rod, and the acceleration was measured as the rod fell. Comparing this acceleration

to one gravity unit, one could determine the friction in the mechanism. Furthermore, the weights were hung at fifteen and thirty degrees to the vertical to give the effect of the horizontal force induced by the model going through the water at various speeds. The results of these tests are tabulated in Table X.

Table X

HEAVE ROD FRICTION

Angle of Weight	Average Friction
0°	.385 lbs.
15°	.506 lbs.
30°	.822 lbs.

To gain insight as to the effect of this friction, a test was conducted at zero speed with the heave rod removed. The model was attached to the towing carriage such that it was free to oscillate on the linear-syn only. It was set to the same amplitude as was used in the heave tests. When the model was released, and the record of the heave compared to that with the heave rod, there was no apparent difference in the response. Accordingly, the effect of heave rod friction was neglected in the final calculations.

As this test was conducted at zero speed and as the weight drop tests showed considerable increase of friction with a horizontal component, this may have been a source of slight error at higher Froude numbers. However, this effect was considered secondary and was neglected.

APPENDIX B

EFFECTS OF WALL REFLECTIONS

A question raised early in the testing was how valid the results would be or whether the effects of wave reflections in a narrow tank would be such as to render the response meaningless. Because of this possibility, two procedures were available to get better results at zero speed. One was to test the model at different orientations in the tank, and if this proved unsuccessful, to make the tests in a larger medium, such as a swimming pool.

The model was first tested parallel to the tank. The heave response obtained is shown in Figure XVII. The model was then tested at an orientation perpendicular to the tank, and the response is shown in Figure XVIII. Similar results were obtained for pitch. In both cases it is noted that the model oscillations damped to zero before any wall reflections affected the motion of the model. It is true that the extremely long waves returned to the model almost instantly, but their effect is negligible, and it is the wave of the same order of magnitude as the ship length with which we are primarily concerned.

It is interesting to note that there is a considerably longer zero region when the model was placed across the tank than when it was oriented parallel to the tank. This indicates that wall reflections must be considered in this type of analysis, but fortunately, for the Mariner model the oscillations completely damped out prior to wall reflections. Thus the results of the analysis were essentially the same for each condition.

FIGURE XVII

ZERO SPEED HEAVE RESPONSE (PARALLEL)

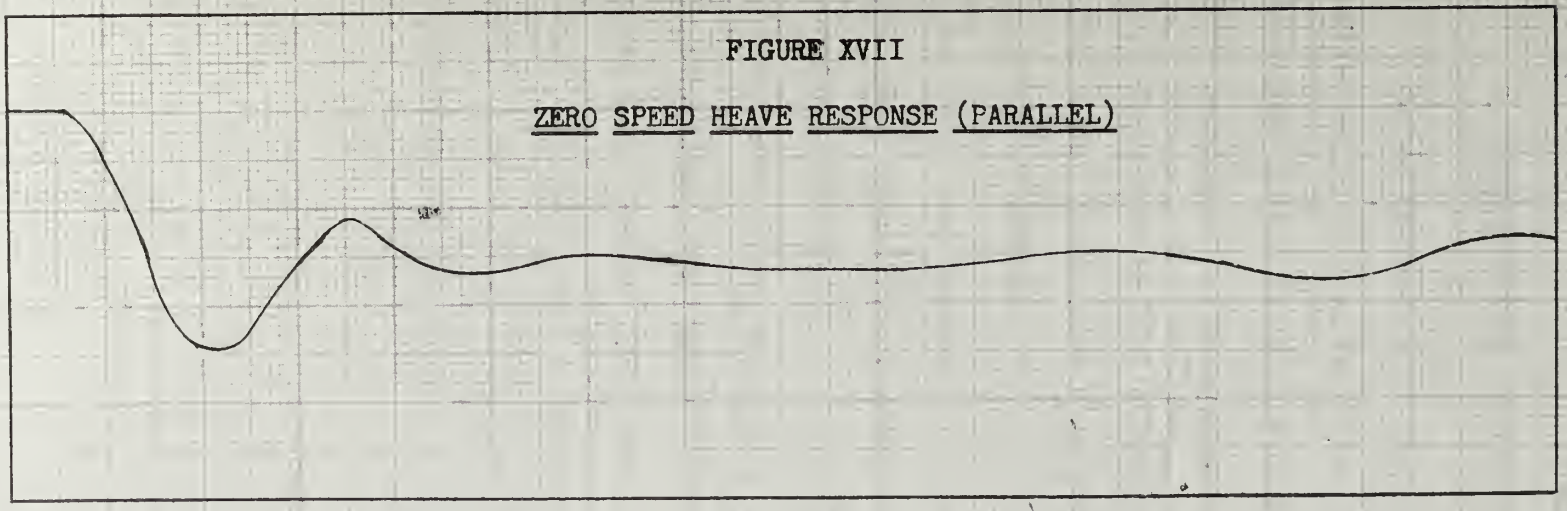

FIGURE XVIII

ZERO SPEED HEAVE RESPONSE (PERPENDICULAR)

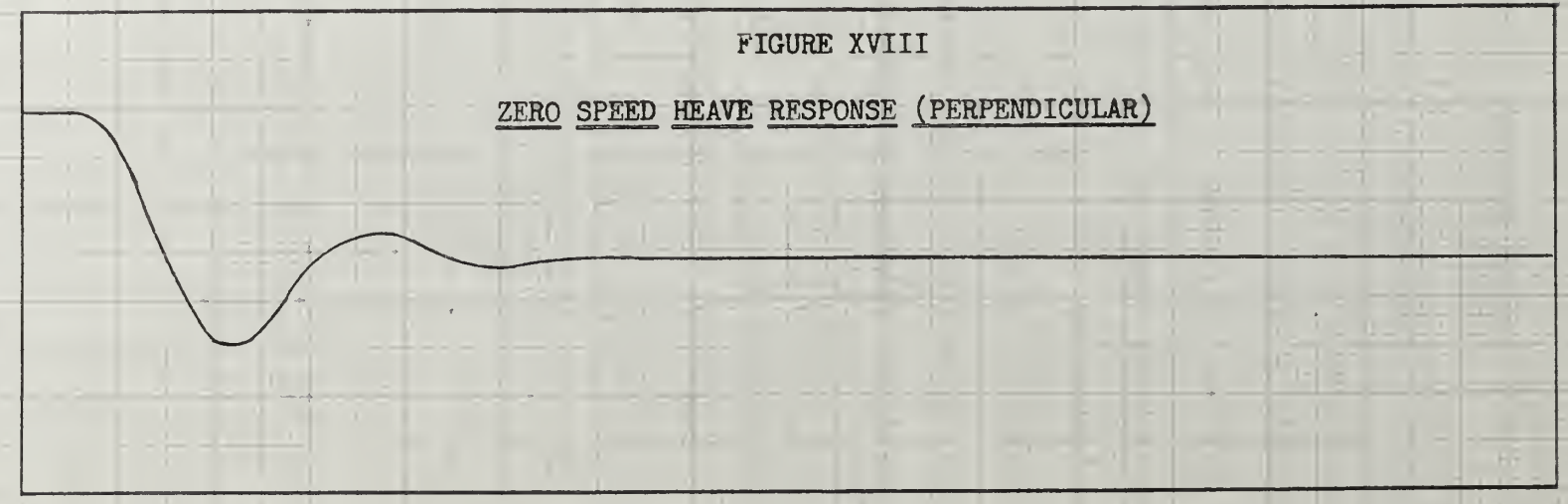

APPENDIX C

DETERMINATION OF COEFFICIENTS OF TRANSFORMATION

The determination of the coefficients of transformation of the semicircle in one complex plane to the ship section in the second complex plane proved to be very adaptable to computer operation. The IBM 7094 computer at the Massachusetts Institute of Technology was used for this purpose in this project. In general, the mapped cylinder gave a very close approximation to the actual ship section. The method used consisted of selecting tentative values of a_1, a_3, and a_5 by reference to Landweber and Macagno (9). The computer program was then entered with these values and offsets of the actual ship section. An iteration procedure written into the program generated new values of the coefficients and offsets which were compared with the actual ship section. The iterations were continued until a reasonably small least mean square error between calculated and actual offsets was obtained. The maximum deviation used in this project occured at station one. Figure XIX in this appendix compares the actual station one with station one derived from the transformation coefficients.

FIGURE XIX

COMPARISON OF THE ACTUAL MARINER STATION ONE WITH THE CALCULATED SECTION

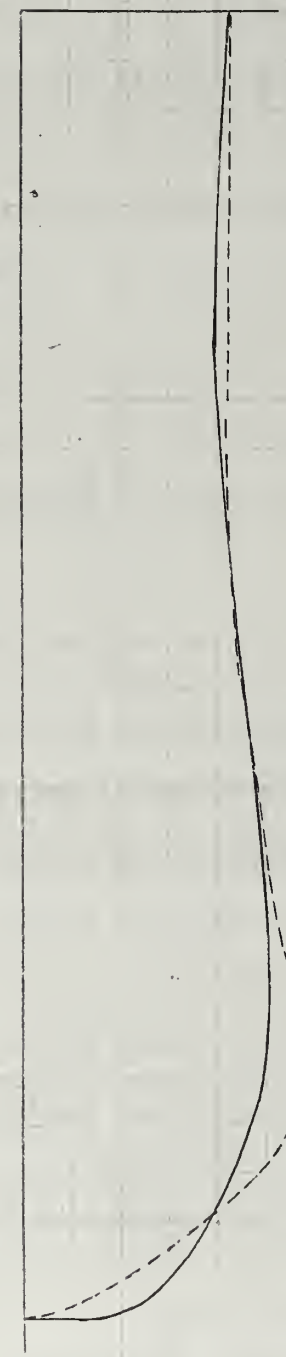

APPENDIX D

NEW METHOD FOR DETERMINATION OF TRANSFORMATION COEFFICIENTS

After the main body of work on this project was completed, a new method for determining the transformation coefficients, a_{2n+1}, was devised. This method, together with the new values of the transformation coefficients for the stations of the Mariner hullform, are presented in this appendix.

Equation (5) represents the conformal transformation of the unit circle to the section in question. In equation (5)

$$\zeta = i\rho e^{-i\theta} \tag{17}$$

$$z = x + iy = ire^{-i\beta} \tag{18}$$

In this work the y axis points down, and the angles θ and β are measured from the vertical. X is the offset of the actual form, and y is the waterline. Therefore, when $\theta = \beta = 90^{\circ}$, x is the half-beam of the section, and $y = 0$. When $\theta = \beta = 0^{\circ}$, $x = 0$, and y is the draft of the section.

By substituting equations (16) and (17) into equation (5) and separating the real and imaginary parts, the following equations are obtained:

$$x = \rho\sin\theta + \sum_{n=0}^{N} (-1)^n \frac{a_{2n+1}}{\rho^{2n+1}} \sin(2n+1)\theta \tag{19}$$

$$y = \rho\cos\theta + \sum_{n=0}^{N} (-1)^{n+1} \frac{a_{2n+1}}{\rho^{2n+1}} \cos(2n+1)\theta \qquad (20)$$

It is then necessary to solve for θ and a_{2n+1} which satisfy these equations.

If M points on a section outline are available, there are M pairs of equations of the above form, or a total of 2M equations. The values of a_{2n+1} must be the same in all of these equations, but the values of θ will be unique for each given point.

If the half-beam and draft of the section are known, an additional equation is available. As mentioned above, at $\theta = 90^{\circ}$,

$$\text{half-beam} = b = \rho + \sum_{n=0}^{N} \frac{a_{2n+1}}{\rho^{2n+1}} \qquad (21)$$

At $\theta = 0^{\circ}$,

$$\text{draft} = H = \rho + \sum_{n=0}^{N} (-1)^{n+1} \frac{a_{2n+1}}{\rho^{2n+1}} \qquad (22)$$

These results lead to the equation

$$\rho\left(1 - \frac{b}{H}\right) + \frac{a_1}{\rho}\left(1 + \frac{b}{H}\right) + \frac{a_3}{\rho^3}\left(1 - \frac{b}{H}\right) + \ldots = 0 \qquad (23)$$

We now have 2M+1 equations which must be satisfied.

In the new method of solving for the coefficients a_{2n+1}, the coordinates of the M points, as well as the half-beam and draft of the

section, are inputs to the computer program. Three alternatives are now available. If estimated values of the coefficients a_{2n+1} are available, they may be entered. In lieu of this, if estimates of the angles θ are available, they may be entered as inputs to the program. If neither the coefficients nor the angles θ are available, the program will generate an estimate of the angles θ.

Assuming that either the angles θ are inputs or that values of θ are internally generated, the program solves the 2M+1 equations for ρ and a_{2n+1} to give a least mean square error solution between the generated section and the actual ship section. The values of the coefficients are then used with input values of x and y to determine a new value of θ for each point. The program then re-enters the least mean square process and iterates until the desired number of iterations is completed. If values of a_{2n+1} are inputs, the program computes values of θ before entering the mean square process.

It should be noted that the program requires the number of coefficients desired and the number of iterations desired as inputs.

As stated above, the program finds values of ρ. However, since we are interested in the case of the unit circle, the program is normalized with ρ equal to one.

Using this new method, new values of a_{2n+1} were determined for the Mariner hullform. These coefficients are presented in Tables XI and XII.

It is believed that this improved approximation to the hullform will not appreciably affect the values of damping and virtual mass for the Mariner. However, in future work it is recommended that the new

method presented above be used.

A listing of the analysis program in MAD computer language is attached to this appendix.

Table XI

TRANSFORMATION COEFFICIENTS

Station	a_1	a_3	a_5	a_7	a_9
0	-.858571	-.118183	-.018627	+.006032	-.000315
1	-.675965	-.085363	-.513534	+.006935	+.005787
2	-.479528	-.043086	+.010433	+.003225	+.013838
3	-.286588	-.022750	+.019479	+.003222	+.016652
4	-.117882	-.020844	+.019821	+.005278	+.010582
5	-.000435	-.035251	+.017899	+.002628	+.007844
6	+.076025	-.053853	+.016527	+.001457	+.005735
7	+.121668	-.078578	+.010747	-.000674	+.002915
8	+.143994	-.102216	+.004109	-.001911	
9	+.150007	-.119040	-.001388	-.002853	
10	+.150031	-.124746	-.004275	-.004280	+.001686
11	+.151144	-.122959	-.003435	-.004104	
12	+.150825	-.110575	-.001117	-.004822	
13	+.148566	-.085017	+.005537	-.004659	
14	+.139671	-.048057	+.016075	-.004566	+.001582
15	+.117410	-.002430	+.024345	-.001183	+.006575
16	+.069663	+.053825	+.032166	+.000042	+.009334
17	-.026949	+.106876	+.043512	-.001900	+.006618
18	-.216518	+.146021	+.074115	+.012576	-.003023
19	-.562587	+.131206	+.098245	+.047890	+.016198
20	+.227269	+.251236	-.124012	+.048271	-.109952

Table XII

COMPARISON OF ERRORS WITH THOSE FOUND BY PROCESS USED IN THE MAIN BODY OF THE PROJECT

	New Method		Main Body	
Station	Average Excursion	Maximum Excursion	Average Excursion	Maximum Excursion
0	0.07	0.11		
1	0.09	0.17	0.32	0.93
2	0.16	0.33	0.17	0.32
3	0.13	0.25	0.20	0.54
4	0.12	0.23	0.11	0.40
5	0.10	0.22	0.13	0.32
6	0.08	0.17	0.08	0.17
7	0.06	0.13	0.06	0.18
8	0.03	0.07	0.07	0.13
9	0.02	0.07	0.02	0.08
10	0.05	0.12	0.08	0.23
11	0.06	0.11	0.06	0.11
12	0.03	0.09	0.03	0.09
13	0.03	0.05	0.04	0.08
14	0.03	0.09	0.04	0.10
15	0.09	0.25	0.19	0.40
16	0.08	0.19	0.24	0.55
17	0.12	0.27	0.19	0.52
18	0.06	0.11	0.22	0.46
19	0.15	0.30	0.29	0.69
20	0.07	0.13	0.07	0.20

```
          RCOEFFICIENT DETERMINATION FOR HULL FORMS
           DIMENSION B(625,BDIM),THETA(625,TDIM),X(30),Y(30),ABAR(25),
          1   APRI(15),BETA(30),CRIT(20),A(15),WYE(30),EX(30),ERRX(30),
          2  ERRY(30),NAME(12),DEGREE(625,DDIM),ALPHA(30),DUM(225,DIMD)
           INTEGER I,J,K,M,N,Q,COUNT,PWR,SIGNAL
           VECTOR VALUES BDIM = 2,1,25
           VECTOR VALUES TDIM = 2,1,25
           VECTOR VALUES DDIM = 2,1,25
           VECTOR VALUES DIMD = 2,1,15
START      READ FORMAT TITL1,NAME(1)...NAME(12)
           VECTOR VALUES TITL1 = $(12C6)*$
           PRINT FORMAT TITL2,NAME(1)...NAME(12)
           VECTOR VALUES TITL2 = $(1H1,12C6)*$
           READ FORMAT INPUT, H,M,N,Q,BEAM,SIGNAL
           VECTOR VALUES INPUT = $(F10.6,3I2,F10.6,I2)*$
           BDIM(2) = N+2
           DIMD(2) = N+1
           TDIM(2) = Q+1
           DDIM(2) = Q+1
           READ FORMAT OFFSET, X(1)...X(M)
           VECTOR VALUES OFFSET = $(5F10.4)*$
           READ FORMAT WL, Y(1)...Y(M)
           VECTOR VALUES WL = $(5F10.4)*$
           KAY = BEAM/H
           E1 = 1.0E-06
           WHENEVER SIGNAL .E. 0
           READ FORMAT ANGLE, EX(1)...EX(M)
           THROUGH BEE1, FOR I = 1,1, I.G.M
BEE1       DEGREE(I,1) = EX(I)
            VECTOR VALUES ANGLE = $(5F10.5)*$
            THROUGH TWENTY, FOR I = 1,1,I.G.M
TWENTY      THETA(I,1) = DEGREE(I,1)/57.295780
            TRANSFER TO TWELVE
           OR WHENEVER SIGNAL .E. 1
           READ FORMAT AVAL, A(1)...A(N)
           VECTOR VALUES AVAL = $(S4,4E14.6)*$
            THROUGH THIRTY, FOR I = 1,2,I.G.(2*N-1)
THIRTY     A(2*I-1) = A(I)
           DEN = 1. + A(1)
            THROUGH FORTY, FOR I = 3,2,I.G.(2*N-1)
FORTY       DEN = DEN + A(I)
            RO = BEAM/DEN
            THROUGH FIFTY, FOR I = 1,2,I.G.(2*N-1)
FIFTY      APRI(I) = A(I)*RO
            TRANSFER TO TWELVE
           OTHERWISE
            CONTINUE
           END OF CONDITIONAL
          R
          R
            THROUGH INITL, FOR I = 1,1,I.G.M
            THETA(I,1) = ATAN.(X(I)/Y(I))
INITL      WHENEVER Y(I) .LE. E1, THETA(I,1) = 1.57080
TWELVE     THROUGH ONE, FOR J = 1,1,J.G.Q
            WHENEVER SIGNAL .E. 1 .AND. J .E. 1, TRANSFER TO  B1
```

```
          R
          R
           THROUGH TWO, FOR I = 1,1, I.G.M
            B(I,1) = SIN.(THETA(I,J))
            B(I,2) = B(I,1)
            B(I,(N+2)) = X(I)
           B((I+M),1) = COS.(THETA(I,J))
           B((I+M),2) = -F((I+M),1)
           B((I+M),(N+2)) = Y(I)
           THROUGH TWO, FOR K = 3,1, K.G.(N+1)
           B(I,K) = ((-1.).P.K)*SIN.(((2*K)-3)*THETA(I,J))
TWO        B((I+M),K) = -((-1.).P.K)*COS.(((2*K)-3)*THETA(I,J))
           THROUGH THREE, FOR K = 1,1,K.G.(N+1)
THREE      B((2*M+1),K) = 1. + ((-1.).P.K)*KAY
           B((2*M+1),(N+2)) = 0.
          R
          R
           EXECUTE GLSQH.(B,ABAR,DUM,(N+1),(2*M+1))
          R
           PRINT RESULTS ABAR(1)...ABAR(N+1)
          R
           RO = ABAR(1)
           THROUGH FOUR, FOR I = 2,1, I.G. (N+1)
FOUR        APRI((2*I)-3) = ABAR(I)
          R
          R
           THROUGH FIVE, FOR I = 1,2, I.G.((2*N)-1)
FIVE       A(I) = APRI(I)/RO
          R
          R
           THROUGH SIX, FOR I = 1,1, I.G.M
            EX(I) = (RO + APRI(1))*SIN.(THETA(I,J))
            PWR = 0
           DEGREE(I,J) = 57.2958*THETA(I,J)
            WYE(I) = (RO-APRI(1))*COS.(THETA(I,J))
            THROUGH SIXPRI, FOR K = 3,2, K.G.((2*N)-1)
            PWR = PWR + 1
           WYE(I) = WYE(I) - ((-1.).P.PWR)*APRI(K)*COS.(K*THETA(I,J))
SIXPRI     EX(I) = EX(I) + ((-1.).P.PWR)*APRI(K)*SIN.(K*THETA(I,J))
           ERRY(I) = .ABS.(WYE(I) - Y(I))
SIX         ERRX(I) = .ABS.(EX(I)-X(I))
          R
          R
           ALPHA(0) = 0.
           BETA(0) = 0.
           THROUGH EIGHT, FOR I = 1,1, I.G.M
           ALPHA(I) = ALPHA(I-1) + ERRX(I)*ERRX(I)
EIGHT      BETA(I) = BETA(I-1) + ERRY(I)*ERRY(I)
          R
          R
           CRIT(J) = SQRT.(ALPHA(M) + BETA(M))
            EXECUTE OUTPT.(J,RO,A,CRIT,X,EX,ERRX,Y,WYE,ERRY,DEGREE,M,N)
           WHENEVER J.E.Q, TRANSFER TO FINIS
          R
          R
```

```
          THROUGH CEE1, FOR I = 1,2, I.G.(2*N-1)
CFE1       PRINT FORMAT ABC, A(I)
           VECTOR VALUES ABC = $(1H ,E14.6)*$
          PRINT FORMAT LMS, CRIT(J)
          VECTOR VALUES LMS = $(21H LEAST MEAN SQUARE = ,F14.6)*$
          PRINT COMMENT $0 MEASURED X(I)      CALCULATED X(I)       X(I)
         1 ERROR       MEASURED Y(I)      CALCULATED Y(I)       Y(I) ERR
         2OR       THETA(I)$
          THROUGH TEN, FOR I = 1,1, I.G.M
TEN        PRINT FORMAT OFVAL, X(I),EX(I),ERRX(I),Y(I),WYE(I),ERRY(I),
         1  DEGREE(I,J)
           VECTOR VALUES OFVAL = $(1H ,F14.6,S5,F14.6,S5,F14.6,S5,
         1  F14.6,S5,F14.6,S5,F14.6,S5,F14.6)*$
          FUNCTION RETURN
          END OF FUNCTION
    MAD
          EXTERNAL FUNCTION (A,X,B,N,M)
          ENTRY TO GLSQH.
          INTEGER I,J,K,N,M
          THROUGH QQ1, FOR I = 1,1, I.G.N
          X(I) = 0.
          THROUGH QQ1, FOR J = 1,1, J.G.M
QQ1       X(I) = X(I) + A(J,I)*A(J,(N+1))
          THROUGH QQ2, FOR I = 1,1, I.G.N
          THROUGH QQ2, FOR J = 1,1, J.G.N
          B(I,J) = 0.
          THROUGH QQ2, FOR K = 1,1, K.G.M
QQ2        B(I,J) = B(I,J) + A(K,I)*A(K,J)
          THROUGH QQ3, FOR I = 1,1, I.G.N
          WHENEVER B(I,I) .E. 0.
          THROUGH QQ4, FOR K = (I+1),1, K.G.N
          THROUGH QQ5, FOR J = I,1, J.G.N
          TEST = B(I,J)
          B(I,J) = B(K,J)
QQ5       B(K,J) = TEST
          TEST = X(I)
          X(I) = X(K)
          X(K) = TEST
QQ4       WHENEVER B(I,I) .NE. 0., TRANSFER TO QQ6
          END OF CONDITIONAL
QQ6       STORE = B(I,I)
          THROUGH QQ7, FOR J = I,1, J.G.N
QQ7       B(I,J) = B(I,J)/STORE
          X(I) = X(I)/STORE
          THROUGH QQ3, FOR K = 1,1, K.G.N
          WHENEVER K.E.I.OR.B(K,I).E.0., TRANSFER TO QQ3
          STORE = B(K,I)
          THROUGH QQ8, FOR J = I,1, J.G.N
          B(K,J) = B(I,J)*STORE - B(K,J)
QQ8       WHENEVER K.L.I, B(K,J) = -B(K,J)
          X(K) = X(I)*STORE - X(K)
          WHENEVER K.L.I, X(K) = -X(K)
QQ3       CONTINUE
          FUNCTION RETURN
          END OF FUNCTION
```